# High-Rate Interpolation of Random Signals From Nonideal Samples

Tomer Michaeli and Yonina C. Eldar, *Senior Member, IEEE*

***Abstract*—We address the problem of reconstructing a random signal from samples of its filtered version using a given interpolation kernel. In order to reduce the mean squared error (MSE) when using a nonoptimal kernel, we propose a high rate interpolation scheme in which the interpolation grid is finer than the sampling grid. A digital correction system that processes the samples prior to their multiplication with the shifts of the interpolation kernel is developed. This system is constructed such that the reconstructed signal is the linear minimum MSE (LMMSE) estimate of the original signal given its samples. An analytic expression for the MSE as a function of the interpolation rate is provided, which leads to an explicit condition such that the optimal MSE is achieved with the given nonoptimal kernel. Simulations confirm the reduction in MSE with respect to a system with equal sampling and reconstruction rates.**

***Index Terms*—Estimation, generalized sampling, interpolation, random processes, Wiener filtering.**

## I. Introduction

We treat the problem of reconstructing a random signal from a sequence of its nonideal samples. The study of sampling random signals was initiated in the late 1950s by Balakrishnan [1]. His well known sampling theorem states that a bandlimited wide sense stationary (WSS) random signal $x(t)$ can be perfectly reconstructed in a mean squared error (MSE) sense from its ideal samples whenever the sampling rate exceeds twice the signal's bandwidth. Reconstruction is achieved by using the sinc function as an interpolation kernel. In practice, though, the signal is never perfectly bandlimited and the sampling device is not ideal, i.e., it does not produce the exact values of the signal at the sampling points. A common situation is that the sampling device integrates the signal, usually over small neighborhoods around the sampling locations. Furthermore, use of the sinc kernel for reconstruction is usually not feasible due to its slow decay.

Balakrishnan's result was later extended by several authors to account for some of its practical limitations. In [2], a sampling theorem for bandpass and multiple-pass WSS signals was developed. It was shown that under certain conditions on the support of the signal's spectrum $\Lambda_{xx}(\omega)$, perfect reconstruction in an MSE sense is possible using an interpolation filter with the same support. This was a first departure from the bandlimited case to broader classes of random signals.

A more general setup is considered in [3], where no limitation on the signal's spectrum is imposed and the sampling device produces nonideal samples, i.e., samples of a filtered version of the signal. Clearly this setting does not always allow for perfect reconstruction. The strategy proposed in [3] is to minimize the MSE between the original and reconstructed signals. A similar setup is also treated in [4] in which a random signal $x(t)$ is estimated from the samples of another random signal $y(t)$. We refer to this system as the hybrid Wiener filter as it operates on a discrete-time signal whereas its output is a continuous-time signal. Reconstruction in the hybrid Wiener setup is obtained by modulating the shifts of a properly designed interpolation kernel with the samples of the signal.

A related problem was treated in [5] where the authors address the problem of designing the interpolation kernel, but from a purely deterministic viewpoint. In this deterministic setting, prior knowledge on the characteristic behavior of the signal is incorporated in the form of a regularization term, which is analogous to the signal's spectrum in the stochastic framework. Interestingly, the reconstruction filter derived in [5] is functionally related to the hybrid Wiener filter, where the inverse of the regularization operator in [5] plays the role of the signal's spectrum in the stochastic formulation.

The expression for the optimal interpolation kernel in the different settings is typically given in the frequency domain, and usually does not have a closed form in the time domain. This limits the applicability of this approach to situations where the kernel needs to be calculated only on a discrete set of points. In this case, the discrete Fourier transform (DFT) can be used to approximate the desired values. Consequently, the hybrid Wiener filter seems to have been used in the image processing community only as a means of enlarging an image by an integer factor [6], [7]. More general geometrical transformations, such as rotation, lens distortion correction, and scaling by an arbitrary factor, were not tackled using this method.

To overcome the difficulties in implementing the hybrid Wiener filter, one may resort to a system that uses a predefined interpolation kernel. In order to obtain a "good" reconstruction in this setup, the signal's samples are processed with a digital correction system prior to reconstruction, as depicted in Fig. 1. Note that the sampling filter $s(-t)$ in the figure is not necessarily bandlimited so that the correction system has to compensate both for the aliasing that occurs in the sampling

Manuscript received September 02, 2007; revised September 01, 2008. First published October 31, 2008; current version published February 13, 2009. The associate editor coordinating the review of this manuscript and approving it for publication was Dr. Chong-Meng Samson See. This work was supported in part by the Israel Science Foundation by Grant 1081/07 and by the European Commission in the framework of the FP7 Network of Excellence in Wireless COMmunications NEWCOM++ (Contract 216715).

The authors are with the Department of Electrical Engineering, Technion-Israel Institute of Technology, Haifa 32000, Israel (e-mail: tomermic@tx.technion.ac.il; yonina@ee.technion.ac.il).

Color versions of one or more of the figures in this paper are available online at http://ieeexplore.ieee.org.

Digital Object Identifier 10.1109/TSP.2008.2008548

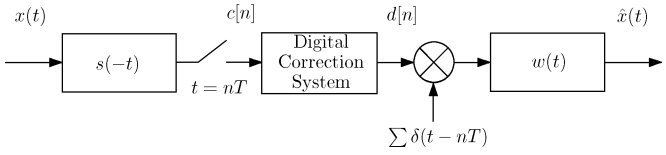


Fig. 1. Sampling and reconstruction setup.

process and for the nonideal interpolation filter. This scheme was first introduced in [8] where the authors considered a stochastic setting. A rigorous treatment of this scheme from a deterministic viewpoint was given in [9]–[12]. In [13] several approaches to design the digital correction filter were developed and compared, including both deterministic and stochastic formulations.

The constraint to a predefined interpolation kernel may lead to severe degradation in the MSE of the reconstruction. This emphasizes the fundamental tradeoff between performance and implementation considerations. An intriguing question that arises, then, is whether one can improve the MSE of such a sampling-reconstruction system by modifying the reconstruction mechanism. In this paper, we suggest compensating for the nonideal behavior of the given interpolation kernel by using a higher reconstruction rate. Specifically, we consider a reconstruction rate that is an integer multiple of the sampling rate $\omega_r = K\omega_s$. This new setting no longer allows the use of a linear time-invariant (LTI) digital correction system but rather forces the use of a multirate digital scheme.

Our proposed framework can be viewed as a generalization of the widely practiced methods for sampling rate conversion, known as first and second order approximation [14]. These methods correspond to a rectangular and a triangular interpolation filter, respectively, and a correction system in the form of a polyphase filter structure. However, besides extending the discussion to general interpolation filters, in this paper, we also relax the standard assumption that the input signal is bandlimited. Furthermore, as stated above, we take a stochastic viewpoint so that we design a correction system that is best adapted to the input signal's spectrum.

Our approach somewhat resembles a scheme proposed in [8], where a multirate digital correction system in the form of an up-sampler followed by a predefined digital filter was designed. However, our work differs from [8] in several aspects. First, we do not pose any restrictions on the digital correction system. Second, in [8] the minimization criterion involves the Fourier transforms of the input and output signals, which is not defined for stationary processes (as a typical realization of a stationary signal is not in $L_2(\mathbb{R})$). This is only possible in [8] since they consider an optical system with a finite-size sensor. Finally, in this paper, we thoroughly study the statistical properties of the reconstructed signal and the effect of the reconstruction rate on the MSE, and show when this scheme produces the optimal hybrid Wiener filter solution.

The paper is organized as follows. In Section II we briefly present the hybrid Wiener filtering problem and its solution. The exposition is different from the classical viewpoint as it is developed in a way that enables the comparison to our approach. We also present the high-rate interpolation strategy and compare it to the hybrid Wiener filter. In Section III we discuss the problematic nature of the MSE as a measure to be minimized in our framework. This motivates the use of an alternative error measure called the average MSE. We further address the well known phenomena of artifacts in the reconstructed signal, caused as a side effect of minimizing the MSE. This is done by studying the statistical properties of the reconstructed signal. In Section IV an explicit expression for the digital correction system as a function of the sampling and reconstruction filters and the signal's spectrum is derived. An error analysis of our scheme is presented in Section V. As a special case we obtain expressions for the MSE in the standard sampling scheme both with a predefined and with the optimal reconstruction kernels. This enables us to address several important issues. First, we derive the optimal sampling filter to be used with a given interpolation kernel. Second, we obtain necessary and sufficient conditions for perfect recovery of a signal from its nonideal samples. Third, we show in what cases our system completely compensates for the nonideal interpolation kernel and produces the minimum MSE solution. We conclude the paper in Section VI, with simulations on synthetic as well as real-world data.

## II. The Hybrid Wiener Filter and the High-Rate Interpolation Scheme

### A. The Hybrid Wiener Filter

We begin by reviewing the hybrid Wiener solution and discuss its application to the recovery of a random signal from its nonideal samples.

The hybrid Wiener filtering problem, in its most general form, is the following. We wish to linearly estimate the WSS random signal $x(t)$ given the equidistant samples of another random signal $y(t)$. The estimate $\widehat{x}(t)$ is chosen such that the MSE $E[|x(t)-\widehat{x}(t)|^2]$ is minimized for every $t$. The spectrum of $y(t)$ and the cross spectrum of $x(t)$ and $y(t)$ are assumed to be known and are denoted by $\Lambda_{yy}(\omega)$ and $\Lambda_{xy}(\omega)$ respectively.[1] The term "hybrid" refers to the fact that the input to the estimator is the discrete-time signal $y(nT)$, $n \in \mathbb{Z}$, whereas the output is a continuous-time signal $\widehat{x}(t)$, $t \in \mathbb{R}$. For notational convenience, we use a normalized sampling period of $T = 1$ throughout the paper.

Interestingly, the solution to this problem highly resembles the standard Wiener filter [15] and is given by [4]

$$\widehat{x}(t) = \sum_{n\in\mathbb{Z}} y(n)w(t-n) \tag{1}$$

where $w(t)$ is an analog filter whose frequency response is

$$W(\omega) = \frac{\Lambda_{xy}(\omega)}{\sum\limits_{l\in\mathbb{Z}} \Lambda_{yy}(\omega_l)} \tag{2}$$

assuming the denominator is nonzero, and

$$\omega_l = \omega + 2\pi l. \tag{3}$$

[1]The cross-spectrum $\Lambda_{xy}(\omega)$ of two jointly WSS signals is the Fourier transform of the cross-correlation function $R_{xy}(\tau) \triangleq E[x(t)y(t-\tau)]$. Setting $x(t) \equiv y(t)$, leads to the definition of the spectrum $\Lambda_{yy}(\omega)$.

As can be seen in (1), the hybrid Wiener solution amounts to a shift-invariant interpolation in between the samples of $y(t)$ using the kernel (2). The denominator of (2) is the discrete-time Fourier transform (DTFT) of the autocorrelation sequence $R_{yy}[n]$ of the samples $y(n)$, i.e., the spectrum[2] $\Lambda_{yy}(e^{i\omega})$ of the discrete-time process $y(n)$. This term replaces the spectrum of the continuous-time signal $y(t)$, which appears in the standard Wiener problem of estimating $x(t)$ from $\{y(t)\}_{t\in\mathbb{R}}$ [15]. We use the notation $\Lambda_{yy}(e^{i\omega})$ to emphasize that the DTFT of a sequence is $2\pi$-periodic.

In our setup, a signal $x(t)$ is sampled after prefiltering by a filter $s(-t)$, which corresponds to the impulse response of the nonideal sampling device. This is described by setting $y(t) = x(t) * s(-t)$. Substituting the appropriate expressions for $\Lambda_{xy}(\omega)$ and $\Lambda_{yy}(\omega)$ in (2), the optimal reconstruction kernel is

$$W(\omega) = \frac{S(\omega)\Lambda_{xx}(\omega)}{\sum\limits_{l\in\mathbb{Z}} |S(\omega_l)|^2 \Lambda_{xx}(\omega_l)}. \tag{4}$$

It is easy to verify that $W(\omega)$ can be chosen arbitrarily for frequencies where the denominator vanishes.

The hybrid Wiener interpolation scheme can be represented in the form of Fig. 1 by choosing the analog filter [5]

$$W_{\rm opt}(\omega) = S(\omega)\Lambda_{xx}(\omega) \tag{5}$$

and the digital filter

$$H_{\rm opt}(e^{i\omega}) = \frac{1}{\sum\limits_{l\in\mathbb{Z}} |S(\omega_l)|^2 \Lambda_{xx}(\omega_l)} \tag{6}$$

where, again, $H_{\rm opt}(e^{i\omega})$ can be chosen arbitrarily for frequencies at which the denominator is zero.

This representation is not unique because multiplication of $W(\omega)$ by any nonvanishing $2\pi$-periodic function can be compensated for by dividing $H(e^{i\omega})$ by the same function. It is, thus, apparent that by inserting the digital correction filter block to the sampling scheme, we effectively create a set of optimal interpolation kernels, instead of just one. Formally stated, an interpolation filter $W(\omega)$ is optimal if there exists a nonvanishing $2\pi$-periodic function $\alpha(e^{i\omega})$ such that

$$W(\omega) = \alpha(e^{i\omega})S(\omega)\Lambda_{xx}(\omega) \quad \forall\omega\in\Omega_c \tag{7}$$

where $\Omega_c$ is defined by

$$\Omega_c \triangleq \left\{\omega : \sum_{l\in\mathbb{Z}} |S(\omega_l)|^2 \Lambda_{xx}(\omega_l) \neq 0\right\}. \tag{8}$$

It can be shown that even if the restriction that the correction system be LTI is removed then (7) is still a necessary condition. A concise statement of this property along with a proof is given in Appendix A.

Equation (7) relates the support of $W(\omega)$ to that of $S(\omega)\Lambda_{xx}(\omega)$, or equivalently, to the support of the spectrum of $y(t) = x(t) * s(-t)$, as $\Lambda_{yy}(\omega) = |S(\omega)|^2\Lambda_{xx}(\omega)$. Specifically, to attain the minimal MSE, $\text{supp}\{\Lambda_{yy}(\omega)\} \subseteq \text{supp}\{W(\omega)\} \subseteq \text{supp}\{\Lambda_{yy}(\omega)\} \cup \Omega_c$. This implies that the reconstructed signal $\widehat{x}(t)$ can only contain frequency components that are present in $y(t)$. Thus, the hybrid Wiener filter does not reproduce any content of the input $x(t)$, that is zeroed out by the sampling filter $S(\omega)$.

[2]The spectrum $\Lambda_{cc}(e^{i\omega})$ of a WSS discrete-time signal $c[n]$ is the DTFT of the autocorrelation sequence $R_{cc}[n] \triangleq E[c[m]c[m-n]]$.

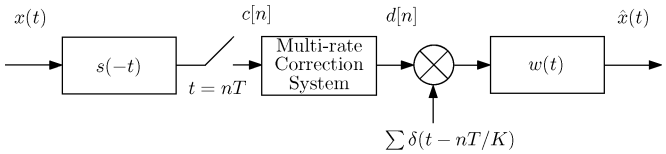


Fig. 2. High rate reconstruction setup.

In Section V we show that when using a high interpolation rate, condition (7) is relaxed, meaning that the set of optimal interpolation kernels is enlarged.

### B. High-Rate Interpolation Scheme

The optimal interpolation filter (5) usually does not admit a closed form in the time domain. We now discuss when this poses a practical problem, and describe an efficient strategy to tackle it.

Consider first resampling applications, such as image enlargement. Here, $\widehat{x}(t)$ needs to be evaluated on a regular grid of points $\{k/\Delta\}_{k\in\mathbb{Z}}$, where $\Delta$ is the magnification factor. In this case (1) becomes

$$\widehat{x}(k/\Delta) = \sum_{n\in\mathbb{Z}} y(n)w_{\rm opt}(k/\Delta - n). \tag{9}$$

If $\Delta$ is an integer, then only a discrete set of samples of $w_{\rm opt}(t)$ plays a role in (9). Thus, $\widehat{x}(k/\Delta)$ is the result of upsampling $y(n)$ by a factor of $\Delta$ and then applying the digital filter $p[n] = w_{\rm opt}(n/\Delta)$. To calculate $p[n]$, we can apply any standard digital filter design method to its Fourier transform $P(e^{i\omega}) = \Delta\sum_{l\in\mathbb{Z}} W_{\rm opt}(\Delta\omega_l)$. The simplest approach would be to sample $P(e^{i\omega})$ on a regular grid of frequencies $\omega = 2\pi m/L$, $m = 0,\ldots,L-1$ and apply the inverse DFT. For $L$ large enough, the resulting sequence is a good approximation of $w_{\rm opt}(n/\Delta)$. This method can also be extended to the case where $\Delta$ is a rational number but with an increase of complexity.

If $\Delta$ is not a rational number then the above method cannot be used directly. However, it can easily be modified to get an approximation of $\widehat{x}(t)$. This is done by first evaluating $\widehat{x}(t)$ on a dense grid, namely computing $\{\widehat{x}(k/K)\}_{k\in\mathbb{Z}}$ with a large integer $K$, and then interpolating in between the grid points using some simple kernel $w(t)$. Commonly, nearest neighbor or linear interpolation are used. These strategies are called first and second order approximation respectively [14]. The resulting scheme is shown in Fig. 2, where the multirate correction system is a $K$-rate up-sampler followed by the digital filter $p[n] = w_{\rm opt}(n/K)$, as depicted in Fig. 3 (right). This multirate system can equivalently be implemented in a polyphase filter structure as shown in Fig. 3 (left). The filter $P(e^{i\omega})$ is related to the polyphase filters $\{H_n(e^{i\omega K})\}_{n=0}^{K-1}$ via [14]

$$P(e^{i\omega}) = \sum_{n=0}^{K-1} H_n(e^{i\omega K})e^{-i\omega n}. \tag{10}$$

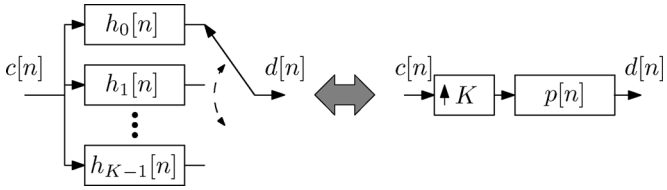


Fig. 3. Two alternative representations of the multirate digital correction system. For every input sample, the commutator in the polyphase structure (left) goes through all $K$ positions, generating $K$ output samples.

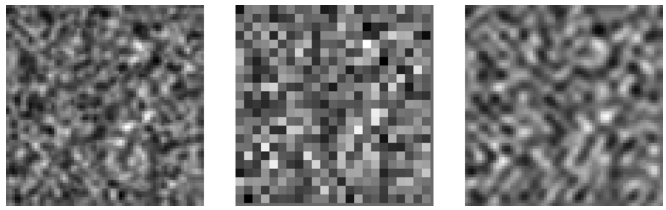

Fig. 4. A stationary 2D random process (left) was downsampled by a factor of 3 and then reconstructed using a rectangular kernel (middle) and the sinc kernel (right).

Clearly, as $K$ tends to infinity this solution approaches the optimal one for any reasonable choice of kernel $w(t)$. However, this system is not optimal in the nonasymptotic regime, as the correction filter $p[n]$ does not compensate for the interpolation to follow. Our goal in this paper is to derive an optimal multirate correction system. This scheme should take into account, not only the signal's spectrum $\Lambda_{xx}(\omega)$ and sampling filter $S(\omega)$ (as in the unconstrained hybrid Wiener filter (5)), but also the predefined reconstruction filter $W(\omega)$.

We remark that the optimal discrete-time compensation filter $P(e^{i\omega})$ will usually not have a closed form in the time domain. Thus to compute $p[n]$, one must use some digital filter design method, as in the case when resampling by an integer factor. The benefit is in being able to handle arbitrary resampling factors by using a simple analog reconstruction filter $w(t)$.

## III. Definition of an Error Measure

As a first step towards deriving a solution to the high-rate reconstruction problem, we first study the statistical properties of the reconstructed signal in the standard case of $K = 1$. This step is crucial in order to pose a proper definition of the error to be minimized.

In [13] the authors show that for a general interpolation kernel, there is no digital correction filter that can minimize the MSE for every $t$. In fact, it can be shown that if a filter is designed to minimize the MSE at a certain time instance $t_0$ then it also minimizes the MSE at times $\{t_0 + k\}_{k\in\mathbb{Z}}$ but not over the whole continuum. Furthermore, we show in this section that generally there does not exist any linear digital correction system (not necessarily a filter) that minimizes the MSE for every $t$.

### A. Average MSE Criterion

The signal $x(t)$ in our setup is assumed to be WSS and, as a consequence, the sequence $c[n]$ in Fig. 1 is a discrete WSS random process. Therefore, if the correction system is a digital filter, as used in [8], [13], then $d[n]$ is also WSS.

The reconstructed signal in our system is given by

$$\widehat{x}(t) = \sum_{n\in\mathbb{Z}} d[n]w(t-n). \tag{11}$$

Signals of this type have been studied extensively in the communication literature in the context of pulse amplitude modulation (PAM). It is a known fact that if the sequence $d[n]$ in (11) is a WSS process then $\widehat{x}(t)$ is generally not WSS but rather wide sense cyclostationary with period 1 [16]. The nonstationary behavior of $\widehat{x}(t)$ is the reason why the pointwise MSE can generally not be minimized for every $t$. To overcome this obstacle we can average the pointwise MSE over one sampling period, as done in [17]. Our error measure is thus the sampling-period-average-MSE, which is defined as

$$\mathrm{MSE} = E\left[\int_{t_0}^{t_0+1} |x(t) - \widehat{x}(t)|^2\, dt\right]. \tag{12}$$

An important property of the above definition is that in situations where the pointwise MSE *can* be minimized for every $t$, the minimization of (12) leads to the same solution. This follows from the fact that the pointwise MSE is nonnegative for every $t$. In Section IV we show that the correction system resulting from the minimization of (12) is independent of $t_0$.

We note that when the signals of interest are natural images or audio signals, there is not a one-to-one correspondence between the MSE of the reconstruction and its quality, as subjectively perceived by the human visual or auditory system. One type of effect which may drastically degrade the subjective quality of the reconstructed signal is due to the nonstationarity of $\widehat{x}(t)$. In fact, if an interpolation scheme outputs a cyclostationary signal when fed with a stationary input, then it will commonly produce reconstructions with degraded subjective quality also when applied to real world signals. We illustrate this in Fig. 4, where a stationary 2D function is downsampled by a factor of 3 and then reconstructed using a rectangular kernel and the sinc kernel. Both interpolation methods lead to the exact same MSE, however the rectangular interpolation filter introduces block structure in the reconstructed image, an artifact which is unpleasant to the human observer. We stress that it is not the scope of this paper to battle these undesired effects. We are merely concerned with the minimization of the MSE. However, it is of interest to study when such artifacts occur. Specifically, we wish to obtain necessary and sufficient conditions on the interpolation kernel and the correction system such that $\widehat{x}(t)$ in (11) is WSS.

### B. Stationarity of the Reconstruction

One example of a WSS PAM signal (11) is when $d[n]$ is WSS and $w(t)$ is the bandlimited filter $w(t) = \mathrm{sinc}(t)$ [16]. An important question is whether this is the only case. We now show that indeed every WSS PAM process is $\pi$-bandlimited. Specifically, for $\widehat{x}(t)$ to be WSS, the following must hold:

1) the sequence $d[n]$ can contain a nonstationary component only if its frequency content is entirely zeroed out by $W(\omega)$;

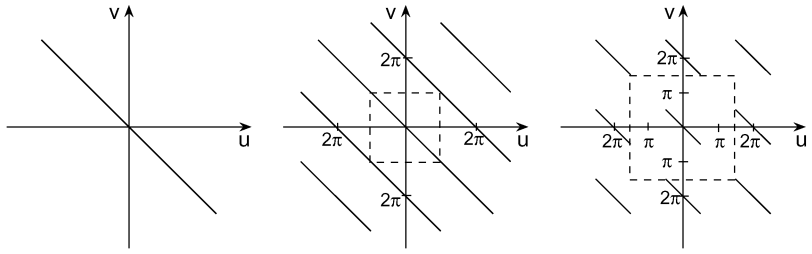


Fig. 5. Left: The spectrum of a WSS process. Middle: The spectrum of $\widehat{x}(t)$ formed by a WSS sequence $d[n]$ with nonvanishing spectrum. Right: The spectrum of $\widehat{x}(t)$ formed by a $(1/2)\pi$-bandlimited WSS sequence $d[n]$.

2) the filter $W(\omega)$ can extend beyond $\pi$ only at frequencies that are not excited by the sequence $d[n]$.

To obtain necessary and sufficient conditions on the sequence $d[n]$ and the filter $w(t)$ such that $\widehat{x}(t)$ is WSS, we compare the two-dimensional spectrum of $\widehat{x}(t)$ with that of a WSS process. We use $\widetilde{R}_{xx}(s,t) = E[x(s)x(t)]$ and $\widetilde{\Lambda}_{xx}(u,v)$ to denote the two-dimensional auto-correlation function of a random signal $x(t)$ and its Fourier transform. If the signal is WSS, then the one-dimensional autocorrelation is denoted $R_{xx}(s) = \widetilde{R}_{xx}(s,0)$ and its Fourier transform is $\Lambda_{xx}(u)$. It is easily verified that for a WSS process, $\widetilde{\Lambda}_{xx}(u,v)$ takes on the form

$$\widetilde{\Lambda}_{xx}(u,v) = \Lambda_{xx}(u)\delta(u+v). \tag{13}$$

Similarly, for a discrete-time WSS signal $z[n]$, the two dimensional spectrum $\widetilde{\Lambda}_{zz}(e^{iu},e^{iv})$ is of the form

$$\widetilde{\Lambda}_{zz}(e^{iu},e^{iv}) = \Lambda_{zz}(e^{iu})\frac{1}{2\pi}\sum_{n\in\mathbb{Z}}\delta(u+v-2\pi n). \tag{14}$$

Now, to determine the conditions for $\widehat{x}(t)$ in (11) to be WSS, we need to identify those cases in which its two-dimensional spectrum is of the form (13). Using (11),

$$\widetilde{R}_{\widehat{x}\widehat{x}}(s,t) = \sum_{m,n\in\mathbb{Z}} w(s-m)w(t-n)\widetilde{R}_{dd}[m,n]. \tag{15}$$

Hence, the spectrum of $\widehat{x}(t)$ can be computed as

$$\begin{aligned}\widetilde{\Lambda}_{\widehat{x}\widehat{x}}(u,v) &= \sum_{m,n\in\mathbb{Z}} \widetilde{R}_{dd}[m,n]W(u)W(v)e^{-imu}e^{-inv}\\ &= W(u)W(v)\widetilde{\Lambda}_{dd}(e^{iu},e^{iv}).\end{aligned} \tag{16}$$

In order for $\widetilde{\Lambda}_{\widehat{x}\widehat{x}}(u,v)$ in (16) to be of the form (13), $\widetilde{\Lambda}_{dd}(e^{iu},e^{iv})$ must be equal to $F(u)\delta(u+v)$ wherever $W(u)W(v) \neq 0$, for some function $F(u)$. However, the function $\Lambda_{dd}(e^{iu},e^{iv})$ is $2\pi$-periodic in each axis as it is a DTFT. Therefore we can only impose $\widetilde{\Lambda}_{dd}(e^{iu},e^{iv}) = F(u)\delta(u+v)$ in the domain $[-\pi,\pi]\times[-\pi,\pi]$. The definition of $\widetilde{\Lambda}_{dd}(e^{iu},e^{iv})$ on the rest of $\mathbb{R}^2$ is then obtained by periodic expansion. This means that $\widetilde{\Lambda}_{dd}(e^{iu},e^{iv})$ must be of the form

$$\widetilde{\Lambda}_{dd}(e^{iu},e^{iv}) = \begin{cases} F(e^{iu})\sum\limits_{n\in\mathbb{Z}}\delta(u+v-2\pi n) & W(u)W(v)\neq 0\\ A(e^{iu},e^{iv}) & W(u)W(v)=0\end{cases} \tag{17}$$

where $A(e^{iu},e^{iv})$ and $F(e^{iu})$ are arbitrary $2\pi$-periodic functions. The top row of (17) is exactly the form of the spectrum of a discrete-time WSS process (14). We conclude that a necessary condition for $\widehat{x}(t)$ to be a WSS continuous-time signal is that $d[n]$ be of the form

$$d[n] = d^S[n] + d^N[n] \tag{18}$$

where $d^S[n]$ is a WSS sequence whose passband is $\{\omega : W(\omega)\neq 0\}$ and $d^N[n]$ is an arbitrary (not necessarily stationary) random sequence whose passband is $\{\omega : W(\omega) = 0\}$. In words, $d[n]$ may exhibit nonstationarity only at frequencies for which $W(\omega)$ vanishes. These frequency components do not affect the reconstructed signal $\widehat{x}(t)$. Therefore, to study the behavior of $\widetilde{\Lambda}_{\widehat{x}\widehat{x}}(u,v)$, we assume in the sequel without loss of generality that $d^N[n] = 0$.

Since $d[n]$ is assumed to be a WSS sequence, its spectrum obeys (14) and thus (16) can be written as

$$\widetilde{\Lambda}_{\widehat{x}\widehat{x}}(u,v) = W(u)W(v)\Lambda_{dd}(e^{iu})\frac{1}{2\pi}\sum_{n\in\mathbb{Z}}\delta(u+v-2\pi n). \tag{19}$$

Fig. 5 (left) depicts the spectrum of a continuous-time WSS signal (13) and that of the reconstructed signal (19) (middle). It is clear that in order for $\widetilde{\Lambda}_{\widehat{x}\widehat{x}}(u,v)$ to possess the form in (13), the impulses outside the line $u+v=0$ have to be suppressed. This happens only if $W(\omega)$ vanishes outside $[-\pi,\pi]$, in which case the content outside the dashed rectangle is supressed. In Fig. 5 (right) we show the spectrum of $\widehat{x}(t)$ formed by a $0.5\pi$-bandlimited WSS sequence $d[n]$. It can be seen that in this case $\widehat{x}(t)$ is WSS if and only if the support of $W(\omega)$ is contained in $[-1.5\pi,1.5\pi]\cup\{[2\pi l+0.5\pi,2\pi l+1.5\pi]\}_{l\in\mathbb{Z}}$. More generally, if $d[n]$ is $B$-bandlimited (where $B\leq\pi$) then the suppression of the undesired impulses can happen only if $W(\omega)$ vanishes outside the set

$$\Omega_W = [-2\pi+B, 2\pi-B]\cup\Omega_d^c \tag{20}$$

where $\Omega_d \triangleq \operatorname{supp}\{\Lambda_{dd}(e^{i\omega})\}$ and the superscript $c$ denotes the complementary of the set. In this case, the reconstructed signal's spectrum is $\Lambda_{\widehat{x}\widehat{x}}(\omega) = (2\pi)^{-1}|W(\omega)|^2\Lambda_{dd}(e^{i\omega})$.

Fig. 6 demonstrates a concrete example of a pair $W(\omega)$, $\Lambda_{dd}(e^{i\omega})$ that forms a WSS signal. In this example the support of $\Lambda_{dd}(e^{i\omega})$ (top) in the interval $[-\pi,\pi]$ is $[-0.75\pi,-0.5\pi]\cup[-0.25\pi,0.25\pi]\cup[0.5\pi,0.75\pi]$ and, hence, $B = 0.75\pi$. The support of $W(\omega)$ (bottom) then must be contained in the union of $[-1.25\pi,1.25\pi]$ and $2\pi$ translates of $[-0.5\pi,-0.25\pi]\cup[0.25\pi,0.5\pi]\cup[0.75\pi,1.25\pi]$.

The following theorem summarizes the results.

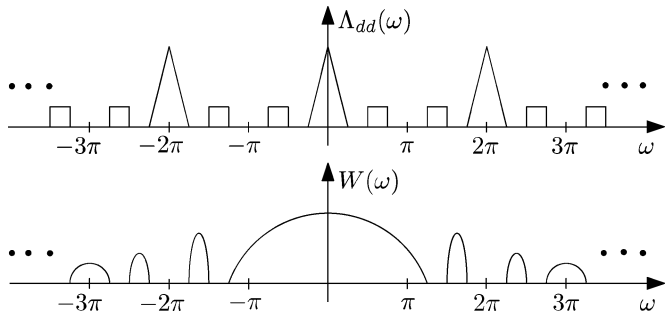


Fig. 6. Example of a pair $W(\omega)$, $\Lambda_{dd}(e^{i\omega})$ that forms a WSS signal.

*Theorem 1:* Consider the signal $\widehat{x}(t)$ in (11). Then $\widehat{x}(t)$ is a continuous-time WSS process if and only if the following hold:

1) the sequence $d[n]$ can be written as $d^S[n]+d^N[n]$, where $d^S[n]$ is a WSS sequence whose passband is $\mathrm{supp}\{W(\omega)\}$ and $d^N[n]$ is an arbitrary random sequence with zero power in $\mathrm{supp}\{W(\omega)\}$;
2) the support of the reconstruction filter $W(\omega)$ is contained in the set $[-2\pi+B, 2\pi-B]\cup\Omega_d^c$, where $B\le\pi$ is the bandwidth of $d[n]$ and $\Omega_d^c$ is the complementary set of the support of $\Lambda_{d^Sd^S}(e^{i\omega})$.

When increasing the reconstruction rate by a factor of $K$, the support of $W(\omega)$ need only be contained in $[-2\pi K, 2\pi K]$ (assuming $B=\pi$), thus a greater class of kernels leads to stationary reconstruction.

Note that the optimal reconstruction kernel $W_{\mathrm{opt}}(\omega)$ of the hybrid Wiener solution (5) generally does not satisfy condition 2. Therefore $\widehat{x}(t)$ is not guaranteed to be stationary when using it. As demonstrated in Fig. 4, this can cause undesired effects in the recovered signal.

## IV. Digital Correction System

In this section we derive an explicit expression for the digital correction system using the error measure (12).

The reconstructed signal in Fig. 2 can be written as

$$\widehat{x}(t)=\sum_{m=0}^{K-1}\sum_{n\in\mathbb{Z}} w\left(t-n-\frac{m}{K}\right)d_m[n] \tag{21}$$

where

$$d_m[n]=\sum_{l\in\mathbb{Z}} h_m[l]c[n-l] \tag{22}$$

is the output of the $m$th filter in Fig. 3. Substituting (22) into (21) leads to

$$\widehat{x}(t)=\sum_{m=0}^{K-1}\sum_{l\in\mathbb{Z}} h_m[l]y_{l,m}(t) \tag{23}$$

where we have defined

$$y_{l,m}(t)\triangleq\sum_{n\in\mathbb{Z}} w\left(t-n-\frac{m}{K}\right)c[n-l]. \tag{24}$$

The average MSE criterion measures the deviation of the process $\widehat{x}(t)$ from $x(t)$ only in the interval $[t_0,t_0+1]$. Let us define an inner product between random processes $a$, $b$ as

$$\langle a,b\rangle=E\left[\int_{t_0}^{t_0+1} a(t)b(t)dt\right]. \tag{25}$$

The induced norm is then $\|a\|^2=\langle a,a\rangle$. We see that the average MSE (12) can be interpreted as the norm of the error process $x(t)-\widehat{x}(t)$. The signal $\widehat{x}(t)$ is a linear combination of $y_{l,m}(t)$. Therefore the error is minimized if and only if the orthogonality principle is satisfied, which implies that $\langle x-\widehat{x}, y_{l,m}\rangle=0$ for every $l\in\mathbb{Z}$, $m=0,\dots,K-1$. Defining the signals $v_m[l]$ and $f_m[l]$ by

$$v_m[l]=E\left[\int_{t_0}^{t_0+1} x(t)y_{l,m}(t)dt\right] \tag{26}$$

$$f_m[l]=E\left[\int_{t_0}^{t_0+1} \widehat{x}(t)y_{l,m}(t)dt\right] \tag{27}$$

we can write the orthogonality condition explicitly as

$$v_m[l]=f_m[l],\quad l\in\mathbb{Z},\ m=0,\dots,K-1. \tag{28}$$

In the following theorem, we show that by converting (28) into the frequency domain, the frequency responses of the $K$ correction filters $h_m[l]$ can be obtained as the solution of a linear system of equations, which is independent of $t_0$.

*Theorem 2:* Let $\boldsymbol{h}(e^{i\omega})$ be the vector consisting of the frequency responses of the $K$ correction filters $h_m[l]$

$$\boldsymbol{h}(e^{i\omega})=\begin{pmatrix}H_0(e^{i\omega}) & \cdots & H_{K-1}(e^{i\omega})\end{pmatrix}^T. \tag{29}$$

Then the vector $\boldsymbol{h}(e^{i\omega})$ minimizing the average MSE (12) is independent of $t_0$ and is given by

$$\boldsymbol{G}(e^{i\omega})\boldsymbol{h}(e^{i\omega})=\boldsymbol{v}(e^{i\omega}). \tag{30}$$

Here $\boldsymbol{G}(e^{i\omega})$ is a $K\times K$ matrix whose $(m,n)$th element is

$$G_{m,n}(e^{i\omega})=\sum_{l\in\mathbb{Z}}|S(\omega_l)|^2\Lambda_{xx}(\omega_l)\sum_{l\in\mathbb{Z}}|W(\omega_l)|^2 e^{i\omega_l\left(\frac{m-n}{K}\right)} \tag{31}$$

$\boldsymbol{v}(e^{i\omega})$ is the $K\times 1$ vector whose elements are

$$V_m(e^{i\omega})=\sum_{l\in\mathbb{Z}} S(\omega_l)\Lambda_{xx}(\omega_l)W^*(\omega_l)e^{i\omega_l\frac{m}{K}}, m=0,\dots,K-1 \tag{32}$$

and $\omega_l=\omega+2\pi l$.

*Proof:* Substituting $\widehat{x}(t)$ of (23) into (27), we have

$$f_m[l]=\sum_{n=0}^{K-1}\sum_{r\in\mathbb{Z}} h_n[r]g_{m,n}[l,r] \tag{33}$$

where we defined

$$g_{m,n}[l,r] = E\left[\int_{t_0}^{t_0+1} y_{r,n}(t)y_{l,m}(t)dt\right]. \quad (34)$$

Now, substituting (24) into this expression, it is shown in Appendix B that $g_{m,n}[l,r]$ is a Toeplitz sequence, i.e., $g_{m,n}[l,r] = g_{m,n}[l-r]$. Therefore the inner sum in (33) reduces to a convolution between $h_n[l]$ and $g_{m,n}[l]$

$$f_m[l] = \sum_{n=0}^{K-1} (h_n * g_{m,n})[l]. \quad (35)$$

This enables us to write (28) in the frequency domain as

$$V_m(e^{i\omega}) = \sum_{n=0}^{K-1} H_n(e^{i\omega})G_{m,n}(e^{i\omega}), \quad m = 0,\ldots,K-1. \quad (36)$$

Explicit expressions for $V_m(e^{i\omega})$ and $G_{m,n}(e^{i\omega})$ are derived in Appendix B, where it is shown that they are both independent of $t_0$ and are given by (31) and (32), respectively. Writing (36) in matrix form leads to (30). ∎

### A. Explicit Formula for the Polyphase Filters

Next we show that it is possible to obtain a closed form solution to (30) by using an orthogonal decomposition of the equations. We also investigate existence and uniqueness of the solution. The explicit expressions for the frequency responses of the $K$ correction filters allows us to obtain a closed form for the MSE of the reconstruction in Section V.

From (31) we see that the matrix $\boldsymbol{G}(e^{i\omega})$ can be written as

$$\boldsymbol{G}(e^{i\omega}) = \sum_{l\in\mathbb{Z}} |S(\omega_l)|^2 \Lambda_{xx}(\omega_l) \sum_{l\in\mathbb{Z}} |W(\omega_l)|^2 \boldsymbol{e}(\omega_l)\boldsymbol{e}^H(\omega_l) \quad (37)$$

where the frequency dependent vector $\boldsymbol{e}(\omega)$ is defined by

$$\boldsymbol{e}(\omega) = \begin{pmatrix} 1 & e^{i\omega\frac{1}{K}} & \cdots & e^{i\omega\frac{K-1}{K}} \end{pmatrix}^T. \quad (38)$$

Therefore $\boldsymbol{G}(e^{i\omega})$ is an infinite weighted sum of rank-one matrices. Similarly, using (32) the vector $\boldsymbol{v}(e^{i\omega})$ can be cast as an infinite weighted sum of vectors

$$\boldsymbol{v}(e^{i\omega}) = \sum_{l\in\mathbb{Z}} S(\omega_l)\Lambda_{xx}(\omega_l)W^*(\omega_l)\boldsymbol{e}(\omega_l). \quad (39)$$

The vector $\boldsymbol{e}(\omega)$ has two interesting properties. First, it is $2\pi K$-periodic in $\omega$. In particular, for every two integers $l$ and $m$ we have $\boldsymbol{e}(\omega_{l+mK}) = \boldsymbol{e}(\omega_l)$. Second, for every $\omega$ the vectors $\boldsymbol{e}(\omega_l), l = 0,\ldots,K-1$ form an orthogonal set: $\boldsymbol{e}^H(\omega_p)\boldsymbol{e}(\omega_q) = K\delta_{p,q}$. These two facts enable us to decompose $\boldsymbol{G}(e^{i\omega})$ into a multiplication of three matrices

$$\boldsymbol{G}(e^{i\omega}) = C_S(e^{i\omega})\boldsymbol{U}(e^{i\omega})\boldsymbol{D}(e^{i\omega})\boldsymbol{U}^H(e^{i\omega}) \quad (40)$$

where $\boldsymbol{U}(e^{i\omega})$ is the orthogonal matrix defined by

$$\boldsymbol{U}(e^{i\omega}) = \begin{pmatrix} \boldsymbol{e}(\omega_0) & \cdots & \boldsymbol{e}(\omega_{K-1}) \end{pmatrix} \quad (41)$$

$\boldsymbol{D}(e^{i\omega})$ is a diagonal matrix containing the values

$$\boldsymbol{D}_{m,m}(e^{i\omega}) = \sum_{l\in\mathbb{Z}} |W(\omega_{m+lK})|^2, \quad m = 0,\ldots,K-1 \quad (42)$$

and $C_S(e^{i\omega})$ is the scalar

$$C_S(e^{i\omega}) = \sum_{l\in\mathbb{Z}} |S(\omega_l)|^2 \Lambda_{xx}(\omega_l). \quad (43)$$

Similarly, the vector $\boldsymbol{v}(e^{i\omega})$ can be written as

$$\boldsymbol{v}(e^{i\omega}) = \boldsymbol{U}(e^{i\omega})\boldsymbol{s}(e^{i\omega}) \quad (44)$$

where the elements of the vector $\boldsymbol{s}(e^{i\omega})$ are given by

$$\boldsymbol{s}_m(e^{i\omega}) = \sum_{l\in\mathbb{Z}} S(\omega_{m+lK})\Lambda_{xx}(\omega_{m+lK})W^*(\omega_{m+lK}). \quad (45)$$

Using (40) and (44), we see that $\boldsymbol{h}(e^{i\omega})$ is the solution to

$$C_S(e^{i\omega})\boldsymbol{U}(e^{i\omega})\boldsymbol{D}(e^{i\omega})\boldsymbol{U}^H(e^{i\omega})\boldsymbol{h}(e^{i\omega}) = \boldsymbol{U}(e^{i\omega})\boldsymbol{s}(e^{i\omega}). \quad (46)$$

*Proposition 1:* There exists a solution to (46) for every $\omega$ regardless of the specific choices of sampling filter $S(\omega)$, reconstruction filter $W(\omega)$ and spectrum $\Lambda_{xx}(\omega)$.

*Proof:* A solution to (46) exists if and only if $\boldsymbol{v}(e^{i\omega})$ lies in the range space of $\boldsymbol{G}(e^{i\omega})$. Let us begin by considering the scalar $C_S(e^{i\omega})$ in (43). If this value vanishes for some $\omega$ then $\boldsymbol{G}(e^{i\omega})$ is the zero matrix. In this case, though, $|S(\omega_l)|^2\Lambda_{xx}(\omega_l) = 0$ for every $l \in \mathbb{Z}$ and, thus, $\boldsymbol{s}_m(e^{i\omega}) = 0$ for every $m$, meaning that $\boldsymbol{v}(e^{i\omega})$ is the zero vector. Therefore, in these situations any $\boldsymbol{h}(e^{i\omega})$ is a solution to (46). Since $C_S(e^{i\omega})$ is the spectrum of the discrete-time process $c[n]$ entering the correction filters, obviously at frequencies where $C_S(e^{i\omega}) = 0$ the frequency responses of the correction filters have no effect on the output signal and can be chosen arbitrarily.

Suppose next that $C_S(e^{i\omega}) \neq 0$. From (40) and (44) it can be seen that $\boldsymbol{v}(e^{i\omega})$ lies in the range space of $\boldsymbol{G}(e^{i\omega})$ if and only if $\boldsymbol{s}_m(e^{i\omega}) = 0$ for every index $m$ where $\boldsymbol{D}_{m,m}(e^{i\omega}) = 0$. However, looking at (42), we see that if $\boldsymbol{D}_{m,m}(e^{i\omega}) = 0$ then $W(\omega_{m+lK}) = 0$ for every $l \in \mathbb{Z}$, which in turn leads to $\boldsymbol{s}_m(e^{i\omega}) = 0$ (45). Therefore, the system of equations (46) is guaranteed to have a solution in this case as well. ∎

Note that there may be frequencies in which there are infinitely many choices of $\boldsymbol{h}(e^{i\omega})$ that satisfy the equations. In the following derivations we choose the vector $\boldsymbol{h}(e^{i\omega})$ with minimal Euclidian norm among all possible solutions.

Using (40) and (44), the minimum norm solution of equation (30) is

$$\begin{aligned}\boldsymbol{h}(e^{i\omega}) &= \boldsymbol{G}^{\dagger}(e^{i\omega})\boldsymbol{v}(e^{i\omega}) \\ &= \frac{1}{K}\boldsymbol{U}(e^{i\omega})\left(C_S(e^{i\omega})\boldsymbol{D}(e^{i\omega})\right)^{\dagger}\boldsymbol{s}(e^{i\omega}) \end{aligned} \quad (47)$$

where we used the fact that $(1/\sqrt{K})\boldsymbol{U}(e^{i\omega})$ is a unitary matrix. The matrix $(C_S(e^{i\omega})\boldsymbol{D}(e^{i\omega}))^\dagger$ is a diagonal matrix whose $m$th diagonal value is given by

$$\begin{cases} \frac{1}{\sum_{l\in\mathbb{Z}}|S(\omega_l)|^2\Lambda_{xx}(\omega_l)\sum_{l\in\mathbb{Z}}|W(\omega_{m+lK})|^2} & \omega\notin\Omega_m \\ 0 & \omega\in\Omega_m \end{cases} \tag{48}$$

where $\Omega_m$ is the set of frequencies for which the denominator does not vanish

$$\Omega_m=\left\{\omega:\sum_{l\in\mathbb{Z}}|S(\omega_l)|^2\Lambda_{xx}(\omega_l)\sum_{l\in\mathbb{Z}}|W(\omega_{m+lK})|^2\neq 0\right\}. \tag{49}$$

Combining (48) and (47) and using the expressions for $\boldsymbol{s}(e^{i\omega})$ (45) and $\boldsymbol{U}(e^{i\omega})$ (41), we obtain the following theorem.

*Theorem 3:* Consider the setup of Theorem 2. Then

$$H_n(e^{i\omega})=\frac{1}{K}\sum_{m=0}^{K-1}\frac{\sum_{l\in\mathbb{Z}}S(\omega_{m+lK})\Lambda_{xx}(\omega_{m+lK})W^*(\omega_{m+lK})}{\sum_{l\in\mathbb{Z}}|S(\omega_l)|^2\Lambda_{xx}(\omega_l)\sum_{l\in\mathbb{Z}}|W(\omega_{m+lK})|^2}e^{\frac{in\omega_m}{K}} \tag{50}$$

where the fraction should be replaced by 0 for frequencies at which the denominator vanishes.

There is an interesting resemblance between (50) and the correction filter developed in [13] for the setup of equal rates of sampling and reconstruction [see (51)]. In (50), the replicas of $S(\omega)\Lambda_{xx}(\omega)W^*(\omega)$ and $|W(\omega)|^2$ are $2\pi K$ apart, whereas in the standard scheme they are $2\pi$ apart. This is due to the increase in interpolation rate by a factor of $K$.

As stated in Section II, an equivalent representation for the multirate correction system is a $K$-rate up-sampler followed by a digital filter $p[n]$. An explicit formula for $P(e^{i\omega})$ can be obtained by substituting (50) in (10).

The special case of reconstruction rate that equals the sampling rate can be easily obtained from (50) by setting $K=1$. In this case, the (single) correction filter is

$$H(e^{i\omega})=\frac{\sum_{l\in\mathbb{Z}}S(\omega_l)\Lambda_{xx}(\omega_l)W^*(\omega_l)}{\sum_{l\in\mathbb{Z}}|S(\omega_l)|^2\Lambda_{xx}(\omega_l)\sum_{l\in\mathbb{Z}}|W(\omega_l)|^2}. \tag{51}$$

This filter coincides with that developed in [13].

## V. Error Analysis

We now analyze the error of the high-rate interpolation scheme. Specifically, we derive a closed form formula for the average MSE of the reconstruction as a function of the interpolation rate $K$, the filters $S(\omega)$ and $W(\omega)$ and the signal's spectrum $\Lambda_{xx}(\omega)$. As a special case, our formula can be used to compute the average MSE in the standard sampling scheme ($K=1$) both for a given interpolation filter $W(\omega)$ and for the optimal one $W_{\rm opt}(\omega)$.

The average MSE of the reconstruction is given by

$$\begin{aligned}\mathrm{MSE}&=E\left[\int_{t_0}^{t_0+1}\left(x(t)-\widehat{x}(t)\right)^2dt\right]\\&=E\left[\int_{t_0}^{t_0+1}\left(x(t)-\widehat{x}(t)\right)x(t)dt\right]\\&=R_{xx}(0)-E\left[\int_{t_0}^{t_0+1}x(t)\widehat{x}(t)dt\right]\end{aligned} \tag{52}$$

where we used the fact that $\widehat{x}(t)$ is orthogonal to the error $x(t)-\widehat{x}(t)$. Using (23), the second term in (52) becomes

$$E\left[\int_{t_0}^{t_0+1}x(t)\widehat{x}(t)dt\right]=\sum_{m=0}^{K-1}\sum_{l\in\mathbb{Z}}h_m[l]v_m[l] \tag{53}$$

where $v_m[l]$ is defined by (26). Using Parseval's relation

$$\begin{aligned}E\left[\int_{t_0}^{t_0+1}x(t)\widehat{x}(t)dt\right]&=\frac{1}{2\pi}\int_{-\pi}^{\pi}\boldsymbol{v}^H(e^{i\omega})\boldsymbol{h}(e^{i\omega})d\omega\\&=\frac{1}{2\pi}\int_{-\pi}^{\pi}\boldsymbol{v}^H(e^{i\omega})\boldsymbol{G}^\dagger(e^{i\omega})\boldsymbol{v}(e^{i\omega})d\omega.\end{aligned} \tag{54}$$

Substituting (54) into the expression for the MSE (52)

$$\mathrm{MSE}=R_{xx}(0)-\frac{1}{2\pi}\int_{-\pi}^{\pi}\boldsymbol{v}^H(e^{i\omega})\boldsymbol{G}^\dagger(e^{i\omega})\boldsymbol{v}(e^{i\omega})d\omega. \tag{55}$$

The second term in (55) can be further simplified using the relations (40) and (44):

$$\begin{aligned}&\boldsymbol{v}^H(e^{i\omega})\boldsymbol{G}^\dagger(e^{i\omega})\boldsymbol{v}(e^{i\omega})\\&\quad=\boldsymbol{s}^H(e^{i\omega})\left(C_S(e^{i\omega})\boldsymbol{D}(e^{i\omega})\right)^\dagger\boldsymbol{s}(e^{i\omega})\\&\quad=\sum_{m=0}^{K-1}\frac{\left|\sum_{l\in\mathbb{Z}}S(\omega_{m+lK})\Lambda_{xx}(\omega_{m+lK})W^*(\omega_{m+lK})\right|^2}{\sum_{l\in\mathbb{Z}}|S(\omega_l)|^2\Lambda_{xx}(\omega_l)\sum_{l\in\mathbb{Z}}|W(\omega_{m+lK})|^2}\end{aligned} \tag{56}$$

where we used the fact that $(C_S(e^{i\omega})\boldsymbol{D}(e^{i\omega}))^\dagger$ is diagonal (48). The fraction in (56) should be replaced by 0 wherever the denominator vanishes. Substituting (56) into (55) we obtain the final expression for the MSE of our interpolation system.

### A. The Standard Sampling Setup With a Predefined Kernel

The standard sampling setup corresponding to $K=1$ was considered in [13] however no explicit formula was given for

the resulting MSE. Setting $K = 1$ in (56) and using (55), the MSE is given by

$$R_{xx}(0) - \frac{1}{2\pi}\int_{-\pi}^{\pi} \frac{\left|\sum_{l\in\mathbb{Z}} S(\omega_l)\Lambda_{xx}(\omega_l)W^*(\omega_l)\right|^2}{\sum_{l\in\mathbb{Z}} |S(\omega_l)|^2 \Lambda_{xx}(\omega_l) \sum_{l\in\mathbb{Z}} |W(\omega_l)|^2} d\omega. \quad (57)$$

In [17, theorem 3] the average MSE of a system with equal rates of sampling and interpolation is analyzed. This scheme comprises given sampling and interpolation filters but, unlike our setup, no digital correction system. Formula (57) can be shown to coincide with [17, theorem 3] if we incorporate the effect of the correction filter into the interpolation kernel and define an effective reconstruction filter as $W_{\text{eff}}(\omega) = H(e^{j\omega})W(\omega)$.

We note that an alternative way of deriving the optimal interpolation filter $W_{\text{opt}}(\omega)$ of (5), is to minimize (57) with respect to $W(\omega)$. This can be done by applying the Cauchy-Schwartz inequality to the numerator of the integrand in (57). Similarly, (57) can be used to determine the optimal sampling filter, when using a predefined interpolation kernel.

*Corollary 4:* Consider estimating a WSS signal $x(t)$ from samples of its filtered version $(x(t) * s(-t))|_{t=n}$ using the interpolation filer $W(\omega)$. Then the minimal MSE is attained if $S(\omega) = \alpha(e^{i\omega})W(\omega)$, where $\alpha(e^{i\omega})$ is an arbitrary $2\pi$-periodic nonvanishing function.

*Proof:* To minimize (57) we have to maximize the integrand with respect to $S(\omega)$. Using the Cauchy-Schwartz inequality

$$\left|\sum_{l\in\mathbb{Z}} S(\omega_l)\Lambda_{xx}(\omega_l)W^*(\omega_l)\right|^2 \le \sum_{l\in\mathbb{Z}} |S(\omega_l)|^2 \Lambda_{xx}(\omega_l) \sum_{l\in\mathbb{Z}} |W(\omega_l)|^2 \Lambda_{xx}(\omega_l) \quad (58)$$

and thus the integrand in (57) is bounded from above by

$$\frac{\sum_{l\in\mathbb{Z}} |W(\omega_l)|^2 \Lambda_{xx}(\omega_l)}{\sum_{l\in\mathbb{Z}} |W(\omega_l)|^2}. \quad (59)$$

It is easily verified that this bound is attained if $S(\omega) = \alpha(e^{i\omega})W(\omega)$, where $\alpha(e^{i\omega}) \neq 0$. ∎

### B. The Hybrid Wiener Filter

The MSE of the hybrid Wiener filter can be calculated from (57) by substituting the optimal reconstruction kernel (5) for $W(\omega)$, resulting in

$$\text{MSE}_{\text{opt}} = R_{xx}(0) - \frac{1}{2\pi}\int_{-\pi}^{\pi} \frac{\sum_{l\in\mathbb{Z}} |S(\omega_l)|^2 \Lambda_{xx}^2(\omega_l)}{\sum_{l\in\mathbb{Z}} |S(\omega_l)|^2 \Lambda_{xx}(\omega_l)} d\omega. \quad (60)$$

The integrand in (60) should be replaced by 0 outside the set $\Omega_c$ defined in (8). In [4] an expression for the pointwise MSE $E[|x(t) - \widehat{x}(t)|^2]$ of the hybrid Wiener filter is derived. The formula given in [4] is different than (60) for two reasons. First, recall that (60) gives the average MSE and not the pointwise MSE. Second, the expression given in [4] is incorrect, since in the derivations of the MSE the author made the implicit assumption that the pointwise MSE is time independent and substituted $t = 0$. Practically, the formula in [4] gives the pointwise MSE at integer times i.e. $E[|x(n) - \widehat{x}(n)|^2]$, $n \in \mathbb{Z}$, but not for the entire continuum.

Equation (60) can be used to study when the high-rate scheme attains the optimal MSE, as done in the next subsection. It can also be used to study in which cases $\text{MSE}_{\text{opt}} = 0$. Not surprisingly, this gives rise to a condition on the passband of $x(t)$, as described in the following corollary.

*Corollary 5:* A WSS signal $x(t)$ with spectrum $\Lambda_{xx}(\omega)$ can be linearly perfectly reconstructed from samples of its filtered version $(x(t) * s(-t))|_{t=n}$ if and only if the following hold:

1) $S(\omega) \neq 0$ for every $\omega \in \text{supp}\{\Lambda_{xx}(\omega)\}$;
2) distinct $2\pi$-shifted replicas of $\Lambda_{xx}(\omega)$ do not overlap, i.e., $\sum_{l\neq 0} \Lambda_{xx}(\omega_l) = 0$, for every $\omega \in \text{supp}\{\Lambda_{xx}(\omega)\}$.

*Proof:* Interchanging the order of integration and summation in the numerator in (60), and making a change of variables $\omega \leftarrow \omega + 2\pi l$, $\text{MSE}_{\text{opt}}$ can be written as

$$\text{MSE}_{\text{opt}} = \frac{1}{2\pi}\int_{-\infty}^{\infty} \left(\Lambda_{xx}(\omega) - \frac{|S(\omega)|^2 \Lambda_{xx}^2(\omega)}{\sum_{l\in\mathbb{Z}} |S(\omega_l)|^2 \Lambda_{xx}(\omega_l)}\right) d\omega. \quad (61)$$

It is easily verified that the integrand in (61) is nonnegative for every $\omega$ and thus $\text{MSE}_{\text{opt}} = 0$ if and only if

$$\Lambda_{xx}(\omega) = \frac{|S(\omega)|^2 \Lambda_{xx}^2(\omega)}{\sum_{l\in\mathbb{Z}} |S(\omega_l)|^2 \Lambda_{xx}(\omega_l)}, \quad a.e.\ \omega \in \mathbb{R}. \quad (62)$$

This condition is trivially satisfied for $\omega \notin \text{supp}\{\Lambda_{xx}(\omega)\}$ as both sides equal zero in this case. For frequencies in $\text{supp}\{\Lambda_{xx}(\omega)\}$ we must demand $S(\omega) \neq 0$ otherwise the right-hand side of (62) would vanish but the left-hand side will not. Now, assuming this condition holds we must have

$$\sum_{l\in\mathbb{Z}} |S(\omega_l)|^2 \Lambda_{xx}(\omega_l) = |S(\omega)|^2 \Lambda_{xx}(\omega) \quad (63)$$

for every $\omega \in \text{supp}\{\Lambda_{xx}(\omega)\}$. Separating out the term $l = 0$, (63) is satisfied if and only if $\sum_{l\neq 0} |S(\omega_l)|^2 \Lambda_{xx}(\omega_l) = 0$ for every $\omega \in \text{supp}\{\Lambda_{xx}(\omega)\}$. But since $S(\omega) \neq 0$ in $\text{supp}\{\Lambda_{xx}(\omega)\}$, this condition becomes

$$\sum_{l\neq 0} \Lambda_{xx}(\omega_l) = 0, \quad \forall \omega \in \text{supp}\,\{\Lambda_{xx}(\omega)\} \quad (64)$$

completing the proof. ∎

A necessary and sufficient condition that allows to perfectly recover a WSS signal from its *ideal* samples was given in [2]. This condition can be obtained as a special case of Corollary 5 by choosing $S(\omega) = 1$. In this case the only requirement is that $2\pi$-translates of the spectrum $\Lambda_{xx}(\omega)$ are disjoint. When the sampling is not ideal we have the additional condition that the sampling filter does not zero out any frequency components contained in $x(t)$.

### C. Optimal Reconstruction Using High Interpolation Rate

An interesting question is when our high-rate interpolation scheme (with a prespecified interpolation filter $W(\omega)$) attains

the optimal MSE. In such cases, our scheme allows to bypass the need for designing the analog interpolation filter without any increase in MSE.

*Theorem 6:* The high-rate interpolation scheme depicted in Figs. 2 and 3 with correction filters given in (50) attains the minimal average MSE attainable by any linear system if and only if there exists a nonvanishing $2\pi K$-periodic function $\alpha(e^{i\omega/K})$ such that

$$W(\omega) = \alpha(e^{i\omega/K})S(\omega)\Lambda_{xx}(\omega) \quad \forall \omega \in \Omega_c \tag{65}$$

where $\Omega_c$ is defined by (8).

*Proof:* From (55), (56), and (60) it can be seen that the difference $\mathrm{MSE} - \mathrm{MSE}_{\mathrm{opt}}$ equals zero if and only if for every $\omega \in \Omega_c$ the following identity holds:

$$\sum_{l\in\mathbb{Z}} |S(\omega_l)|^2 \Lambda_{xx}^2(\omega_l) = \sum_{m=0}^{K-1} \frac{\left|\sum_{l\in\mathbb{Z}} S(\omega_{m+lK})\Lambda_{xx}(\omega_{m+lK})W^*(\omega_{m+lK})\right|^2}{\sum_{l\in\mathbb{Z}} |W(\omega_{m+lK})|^2}. \tag{66}$$

Splitting the sum in the left hand term into $K$ sums, we have

$$\sum_{m=0}^{K-1} \left( \|a_{m,\omega}\|_{l_2}^2 - \frac{|\langle a_{m,\omega}, b_{m,\omega}\rangle|^2}{\|b_{m,\omega}\|_{l_2}^2} \right) = 0 \tag{67}$$

where we denoted $a_{m,\omega}[l] = S(\omega_{m+lK})\Lambda_{xx}(\omega_{m+lK})$ and $b_{m,\omega}[l] = W(\omega_{m+lK})$. From the Cauchy-Schwarz inequality we know that each of the $K$ terms in this sum are nonnegative. Therefore the sum equals zero if and only if each of the $K$ terms equals zero. The Cauchy-Schwarz theorem also states that equality is attained if and only if the sequences $a_{m,\omega}[l]$ and $b_{m,\omega}[l]$ are linearly dependent. This means that there exist $K$ nonvanishing functions $\alpha_m(\omega)$, $m = 0, \ldots, K-1$ such that

$$W(\omega_{m+lK}) = \alpha_m(\omega)S(\omega_{m+lK})\Lambda_{xx}(\omega_{m+lK}) \quad \forall \omega \in \Omega_c \tag{68}$$

for every $l \in \mathbb{Z}$. Condition (68) is identical to (65). ■

Condition (65) is a generalization of (7), which was developed for $K = 1$. This condition implies that an interpolation filter $W(\omega)$ is optimal if and only if it is the product of $S(\omega)\Lambda_{xx}(\omega)$ and some nonvanishing $2\pi K$ periodic function. This gives the essential justification of using the high-rate reconstruction scheme. Specifically, the set of optimal kernels becomes larger as the interpolation rate is increased. In practice, for a large enough rate one may use almost any reasonable interpolation kernel and attain an MSE which is very close to $\mathrm{MSE}_{\mathrm{opt}}$.

When $W(\omega)$ satisfies (65), the high-rate interpolation scheme not only minimizes the average MSE but also the pointwise MSE. This can be shown by repeating the proof of Theorem 7 in Appendix A, for the high rate case.

To illustrate the strength of our method, consider the case in which the input signal $x(t)$ is $B$-bandlimited, i.e. $\Lambda_{xx}(\omega) = 0$, $|\omega| > B$, where $B$ may be greater than $\pi$. In this case the optimal interpolation kernel $W_{\mathrm{opt}}(\omega)$ of the hybrid Wiener filter is a lowpass filter with cutoff frequency $B$. Now, suppose that $W_{\mathrm{opt}}(\omega)$ is hard to implement. From (65) we see that any $B$-bandlimited reconstruction filter $W(\omega)$ can be used to attain the minimal MSE given that it does not vanish in the support of $S(\omega)\Lambda_{xx}(\omega)$ and that the interpolation rate satisfies $K \geq B/\pi$. This is because in this case $2\pi K \geq 2B$ and thus any such $W(\omega)$ can be written as a multiplication of $S(\omega)\Lambda_{xx}(\omega)$ and a nonvanishing $2\pi K$ periodic function. We conclude that for bandlimited input signals it is possible to attain the minimal MSE with *any bandlimited reconstruction kernel* that does not vanish in the support of $W_{\mathrm{opt}}(\omega)$, simply by increasing the reconstruction rate.

## VI. Simulations

### A. Synthetic Data

In order to confirm the efficiency of our proposed scheme, we generated a discrete-time Gaussian random process $x[n]$, filtered it with a prefilter $s[-n]$ and then down sampled it with sampling period $T = 24$ to obtain a sequence of samples $c[n]$. The spectrum $\Lambda_{xx}(e^{i\omega})$ of the signal $x[n]$ is shown in Fig. 7(a) on a frequency axis scaled to $[-24\pi, 24\pi]$. This spectrum contains 5% of its energy outside the interval $[-\pi, \pi]$, which means that no significant aliasing occurs in the sampling process. The sampling filter used was a rectangular filter of length $T$, as depicted in Fig. 7(b). This filter is a good model for an optical system in which the effect of the point spread function (PSF) of the lens is negligible with respect to pixel size.

Our purpose was to reconstruct the original signal using the prespecified interpolation kernel $w[n]$ shown in Fig. 8(a), which corresponds to linear terpolation with period $T$. The filter $w[n]$ has a fast decay with respect to the optimal interpolation kernel, which is depicted in Fig. 8(b). Fig. 9(a) shows the MMSE reconstruction with an interpolation period that equals the sampling period $T$ (i.e., $K = 1$) and with the correction filter (51), as proposed in [13]. Fig. 9(b)–(d), depict the reconstructions obtained by the high-rate interpolation scheme proposed in this paper for $K = 2$, $K = 3$ and $K = 24$ respectively. It can be seen that for low reconstruction rates, the interpolated signal exhibits artifacts in the form of noncontinuity of its derivative. As the reconstruction rate increases, these undesired effects become less dominant. The result in Fig. 9 is exactly identical to the reconstruction that is obtained using the optimal interpolation kernel (with a reconstruction period of $T$).

Fig. 10(a) shows the average MSE attained by the high-rate interpolation scheme as a function of $K$. The dashed line is $\mathrm{MSE}_{\mathrm{opt}}$ of the hybrid Wiener filter. The MSE of the standard sampling scheme $(K = 1)$ is roughly 30% higher than $\mathrm{MSE}_{\mathrm{opt}}$. However, an increase of the interpolation rate by a factor of $K = 3$ is enough to close most of the gap in this case.

Fig. 10(b) shows the pointwise MSE of the hybrid Wiener filter as a function of time. This figure illustrates that even when using the optimal interpolation kernel, the reconstructed signal may be highly nonstationary. In this case the pointwise MSE at times $\{lT\}_{l\in\mathbb{Z}}$ is lower than the pointwise MSE at times $\{(l + 1/2)T\}_{l\in\mathbb{Z}}$ by a factor of 18. As explained in Section III, this can cause undesired artifacts in images or audio signals. One could eliminate this effect by using an interpolation kernel that is $\pi$-bandlimited. Nevertheless, while suppressing nonstationarity, this would result in a higher MSE.

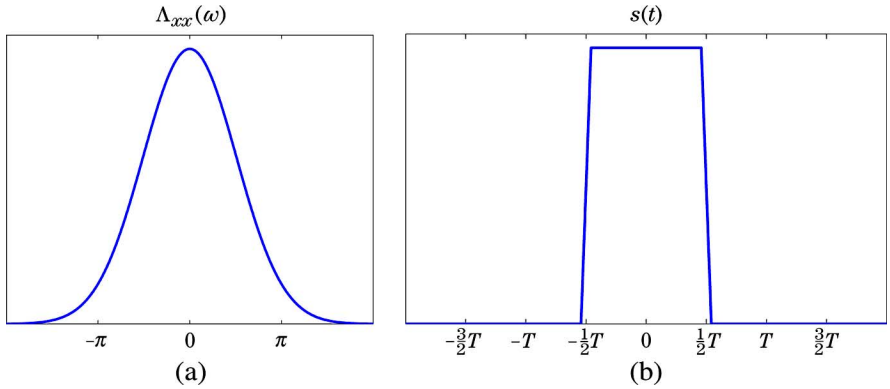


Fig. 7. (a) Spectrum of $x[n]$ on a frequency axis scaled to $[-24\pi, 24\pi]$. An amount of 5% of the energy is concentrated at frequencies above $\pi$. (b) Sampling filter.

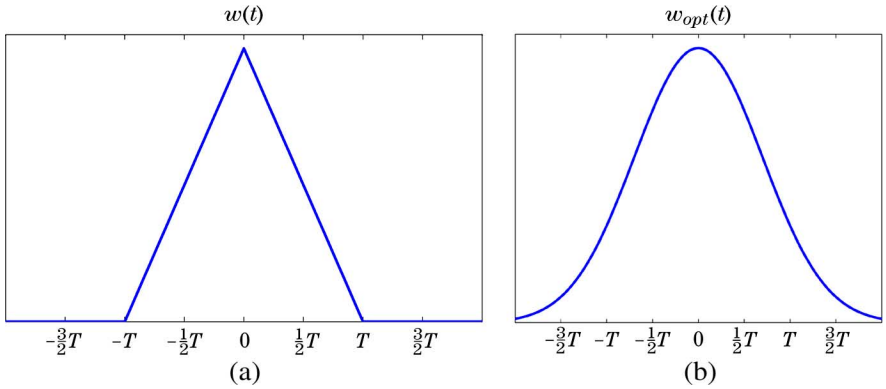


Fig. 8. (a) Given interpolation kernel. This kernel corresponds to linear interpolation for an interpolation rate that equals the sampling rate $T$. (b) Optimal interpolation kernel.

The behavior of the sequence $\mathrm{MSE}(K)$ can be characterized by two properties: its asymptotic value and its rate of convergence to this value. One factor that has a significant contribution to the asymptotic value $\mathrm{MSE}_{\mathrm{opt}}$ is the extent to which aliasing occurs. To illustrate this we repeated the above experiment with a signal $x[n]$ whose portion of energy outside the frequency set $[-\pi, \pi]$ is 20% (as opposed to 5% in the first example). Fig. 11(a) depicts $\mathrm{MSE}(K)$, where it can be seen that $\mathrm{MSE}_{\mathrm{opt}}$ has increased substantially with respect to Fig. 10.

While the asymptotic value $\mathrm{MSE}_{\mathrm{opt}}$ has changed in this last example, the rate of convergence was not affected. The factor that most affects the convergence rate is the resemblance of the prespecified interpolation filter $W(\omega)$ to the optimal one $W_{\mathrm{opt}}(\omega)$. To show this we repeated the first experiment with a rectangular interpolation filter, which is identical to the sampling filter shown in Fig. 7(b). This filter clearly has less resemblance to the optimal filter shown in Fig. 8(b) than the linear interpolation used in the last example. Fig. 11(b) depicts $\mathrm{MSE}(K)$ in this case. It can be seen that the initial value MSE(1) has increased and the rate of convergence has decreased with respect to Fig. 10(a). In this situation, a value of at least $K = 6$ is needed to close most of the gap to the optimal interpolation.

### B. Image Interpolation

We now demonstrate our approach in the context of image interpolation. This requires the specification of the spectrum of the underlying (continuous-space) image. In [6] and [7] it has been found that natural images can be quite accurately modelled as Matern processes. We adopt this assumption here and use the isotropic 2-D Matern spectrum, given by

$$\Lambda_{xx}(\boldsymbol{\omega}) = \frac{\sigma^2}{(\alpha + \|\boldsymbol{\omega}\|^2)^{\nu+1}} \tag{69}$$

where $\boldsymbol{\omega}$ is the 2-D frequency, $\sigma^2$ is proportional to the variance of the process, $\alpha$ defines the effective autocovariance range and $\nu$ controls the smoothness of the signal. The parameters of the model can be estimated from the digital image at hand (the sampled signal $c[\boldsymbol{n}]$), as done in [6] and [7]. However, we have found that using $\nu = 0.3$ and $\alpha = (0.01\pi)^2$ works quite well for natural images. Note that the scaling $\sigma^2$ does not affect the correction filters (50). These values are very similar to the ones reported in [6] and [7].

The second ingredient needed for our system is the sampling filter $S(\boldsymbol{\omega})$. We assume that the value of each pixel is the integration of the continuous-space image over a rectangular domain. Thus, we model $S(\boldsymbol{\omega})$ as the 2-D version of the filter in Fig. 7(b).

Using the above assumptions, the hybrid Wiener interpolation kernel $W_{\mathrm{opt}}(\boldsymbol{\omega})$ (5) can be calculated in the frequency domain, however it does not have a closed form in the space domain. This poses no limitation if the reconstructed image is to be evaluated only on a regular grid of points spaced $1/L$ apart from one another, where $L$ is an integer. Then, the kernel $w(\boldsymbol{t})$ need only be calculated at a discrete set of points, which can be done approximately using DFT. This is the situation when

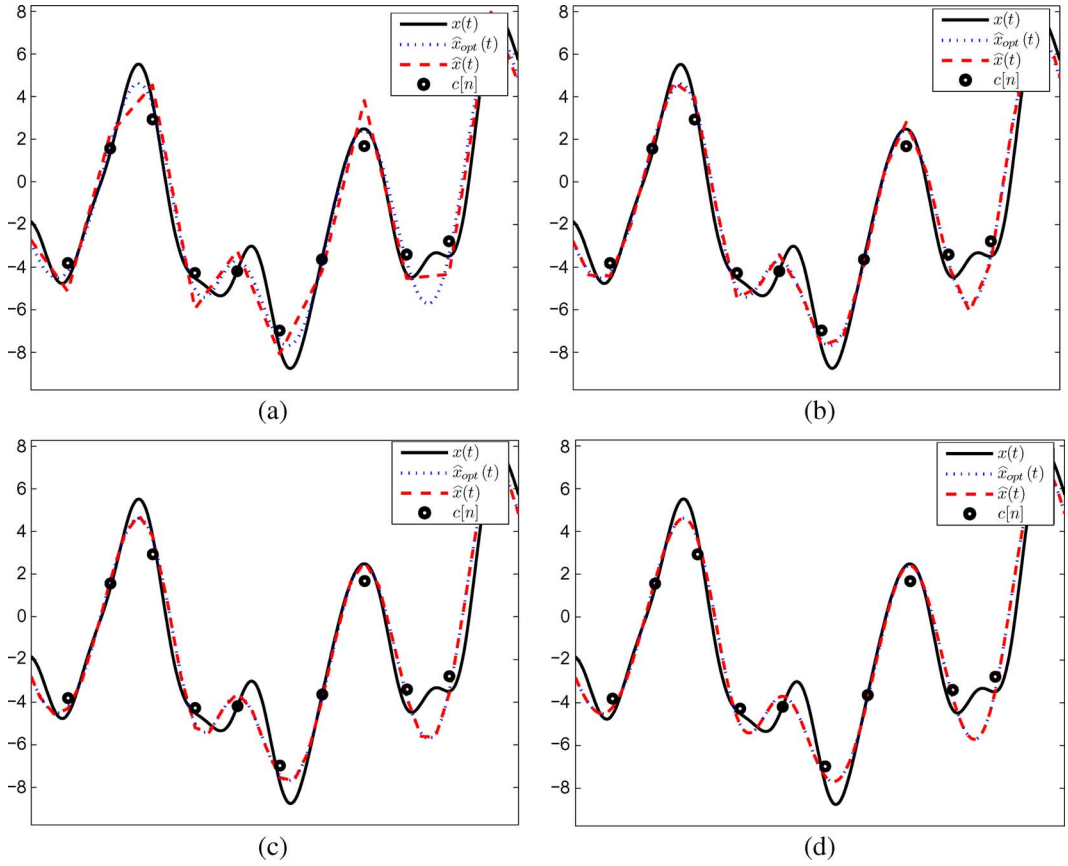


Fig. 9. Reconstructed signal for various interpolation rates. The solid line is the original signal and the circles are the nonideal samples. The dotted and dashed lines correspond to the hybrid Wiener solution and the high rate scheme with the kernel in Fig. 8(a). (a) $K = 1$. (b) $K = 2$. (c) $K = 3$. (d) $K = 24$. In this case the high rate solution coincides with the hybrid Wiener.

enlarging an image by an integer factor, as studied in [6], [7]. However, to apply more general geometrical transformations, such as rotation and scaling by an arbitrary factor, a method to calculate $w(\boldsymbol{t})$ at arbitrary points is needed. In the absence of such method, we must resort to using a predefined interpolation kernel, whose formula in the space domain is available.

One very common alternative to the hybrid Wiener filter is bicubic interpolation. Fig. 12(b) shows the result of enlarging the Mandrill image in Fig. 12(a) by a factor of $\pi/e \approx 1.1557$ using bicubic interpolation. It can be seen that this method tends to blur the fine textures and sharp edges in the image.

Another approach to tackling the problem is to use first or second order approximation [14] to the hybrid Wiener filter. This means we first evaluate the hybrid Wiener solution on a finer grid (i.e. enlarge the image by an integer factor with the kernel $W_{\rm opt}(\boldsymbol{\omega})$) and then use nearest neighbor or linear interpolation to obtain the reconstructed signal at the desired locations. The drawback of this method is that the first stage does not take into account the interpolation to be preformed in the second stage. Fig. 12(c) shows the result of using second order approximation to the Wiener solution evaluated at a grid with 0.5 pixel spacing. As can be seen, the result bears overwhelming resemblance to that in Fig. 12(b). Therefore, in practice, this approach fails to enjoy the advantages of the hybrid Wiener filter.

The high-rate interpolation system proposed in this paper is designed to optimally take into account the interpolation filter. We used our approach with interpolation period of 0.5 pixels and with a kernel corresponding to linear interpolation in the fine resolution. The result is shown in Fig. 12(d). As can be seen, the edges are sharper and the texture is better preserved.

## VII. Conclusion

In this paper, we suggested a scheme for reconstruction of WSS random signals from their nonideal samples using a prespecified interpolation kernel. Our scheme uses an interpolation rate which is higher than the sampling rate in order to compensate for the nonideal interpolation kernel. A multirate digital system that processes the samples prior to multiplying the shifts of the interpolation kernel was developed. We compared the performance of our proposed scheme to the hybrid Wiener filter scheme (in which one is allowed to design the interpolation kernel). This was done by deriving closed form expressions for the MSE of both methods. Specifically, we showed that in our scheme the class of interpolation kernels that allow to attain $\mathrm{MSE}_{\rm opt}$ of the hybrid Wiener filter becomes larger as the reconstruction rate is increased. This means that practically, almost any reasonable interpolation kernel can be used provided that the reconstruction rate is high enough. We also derived necessary and sufficient conditions that allow for perfect reconstruction (in an MSE sense). This result generalizes a known theorem for ideal samples.

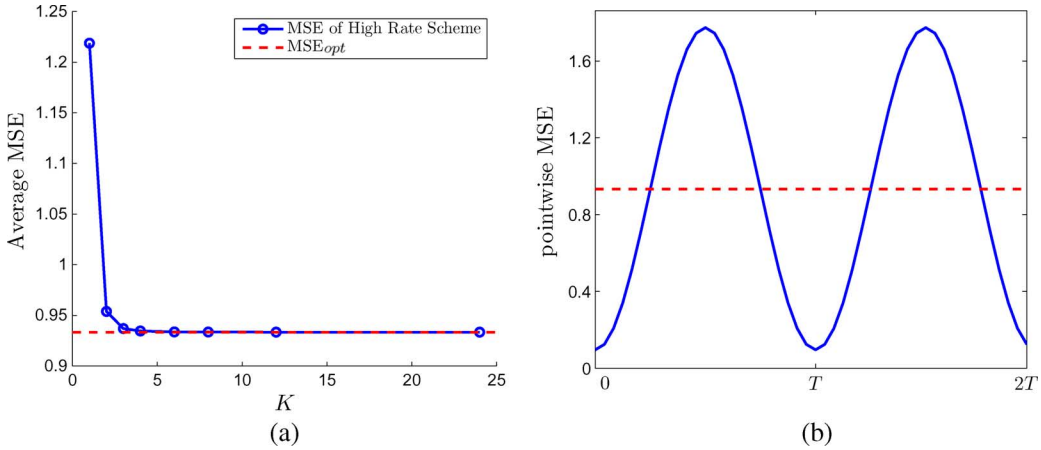


Fig. 10. (a) Average MSE as a function of $K$ for a signal with the spectrum depicted in Fig. 7(a) (1% aliasing) and interpolation filter shown in Fig. 8(b) (b) Pointwise MSE as a function of time for interpolation with the optimal reconstruction kernel.

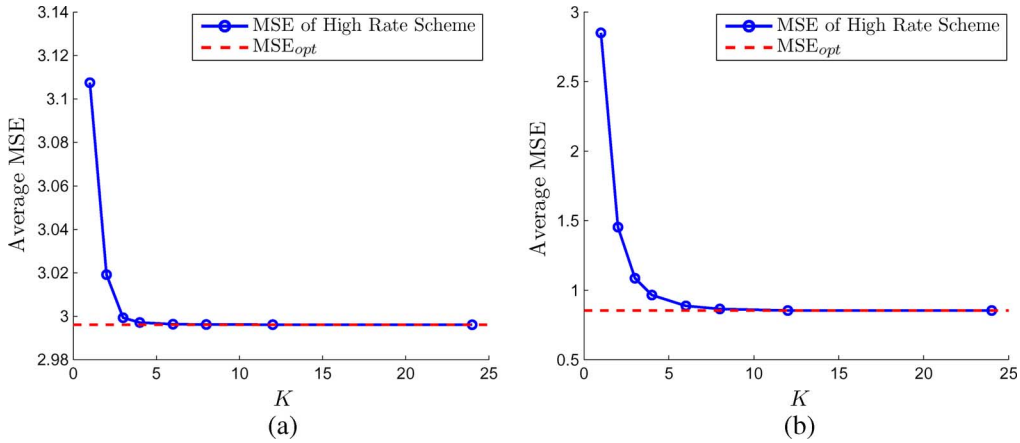


Fig. 11. Average MSE as a function of $K$ for two different setups. (a) A signal with 20% concentration of energy above the frequency $\pi$ and the interpolation filter shown in Fig. 8(a). (b) A signal with 5% concentration of energy above the frequency $\pi$ and the interpolation filter shown in Fig. 7(b).

## APPENDIX A
## NON-LTI DIGITAL CORRECTION SYSTEMS

*Theorem 7:* Let $\widehat{x}(t) = \sum_{n\in\mathbb{Z}} d[n]w(t-n)$, where the sequence $d[m] = \sum_{n\in\mathbb{Z}} h[m,n]c[n]$ is the output of a linear system operating on the samples $c[n] = (x(t) * s(-t))|_{t=n}$. Then the pointwise MSE between $\widehat{x}(t)$ and $x(t)$ is minimized for every $t$ if and only if the following hold:

1) there exists a nonvanishing $2\pi$-periodic function $\alpha(e^{i\omega})$ such that $W(\omega) = \alpha(e^{i\omega})S(\omega)\Lambda_{xx}(\omega)$ for every $\omega \in \Omega_c$, with $\Omega_c$ given by (8);
2) the correction system $h[m,n]$ can be written as $h^{TI}[m-n]+h^{N}[m,n]$, where $h^{TI}[n]$ corresponds to an LTI system $H^{TI}(e^{i\omega}) = (\Lambda_{cc}(e^{i\omega})\alpha(e^{i\omega}))^{-1}$ for every $\omega \in \Omega_c$, and $h^{N}[m,n]$ is an arbitrary (not necessarily LTI) system that satisfies $H(e^{iv}, e^{iu}) = 0$ for every $v \in \Omega_c$ and arbitrary $u$.

Before providing a proof, note that Theorem 7 implies that the nonstationary component of $d[n]$ can only contain frequencies that are suppressed by $W(\omega)$ and, thus, do not affect $\widehat{x}(t)$. The simplest way of enforcing condition 2 is confining the discussion to LTI systems for which $h^{N}[m,n] = 0$. In this case, condition 1 coincides with (7).

*Proof:* A necessary and sufficient condition for the signal $\widehat{x}(t)$ to minimize the pointwise MSE to $x(t)$ is that the orthogonality principle is satisfied for every $t$. Specifically, the error $x(t) - \widehat{x}(t)$ has to be orthogonal to each of the nonideal samples $c[n] = (x(t) * s(-t))|_{t=n}$, i.e.

$$E\left[(x(t) - \widehat{x}(t))\, c[m]\right] = 0, \quad m \in \mathbb{Z},\ t \in \mathbb{R}. \tag{70}$$

Substituting the expression for $\widehat{x}(t)$ in terms of $d[n]$, this condition becomes

$$E\left[x(t)c[m]\right] = \sum_{n\in\mathbb{Z}} R_{cd}[m,n]w(t-n), \quad m \in \mathbb{Z},\ t \in \mathbb{R} \tag{71}$$

where $R_{cd}[m,n] = E[c[m]d[n]]$ is the cross-correlation sequence of the processes $c[n]$ and $d[n]$. In Appendix B, it is shown that $E[x(t)c[m]] = (R_{xx}(t) * s(t))(t-m)$. Substituting this term into (71) and taking the continuous-time Fourier transform (with respect to $t$) we get

$$\begin{aligned}\Lambda_{xx}(v)S(v)e^{-ivm} &= \sum_{n\in\mathbb{Z}} R_{cd}[m,n]W(v)e^{-ivn} \\ &= W(v)\mathcal{F}\left\{R_{cd}[m,\cdot]\right\}(e^{iv})\end{aligned} \tag{72}$$

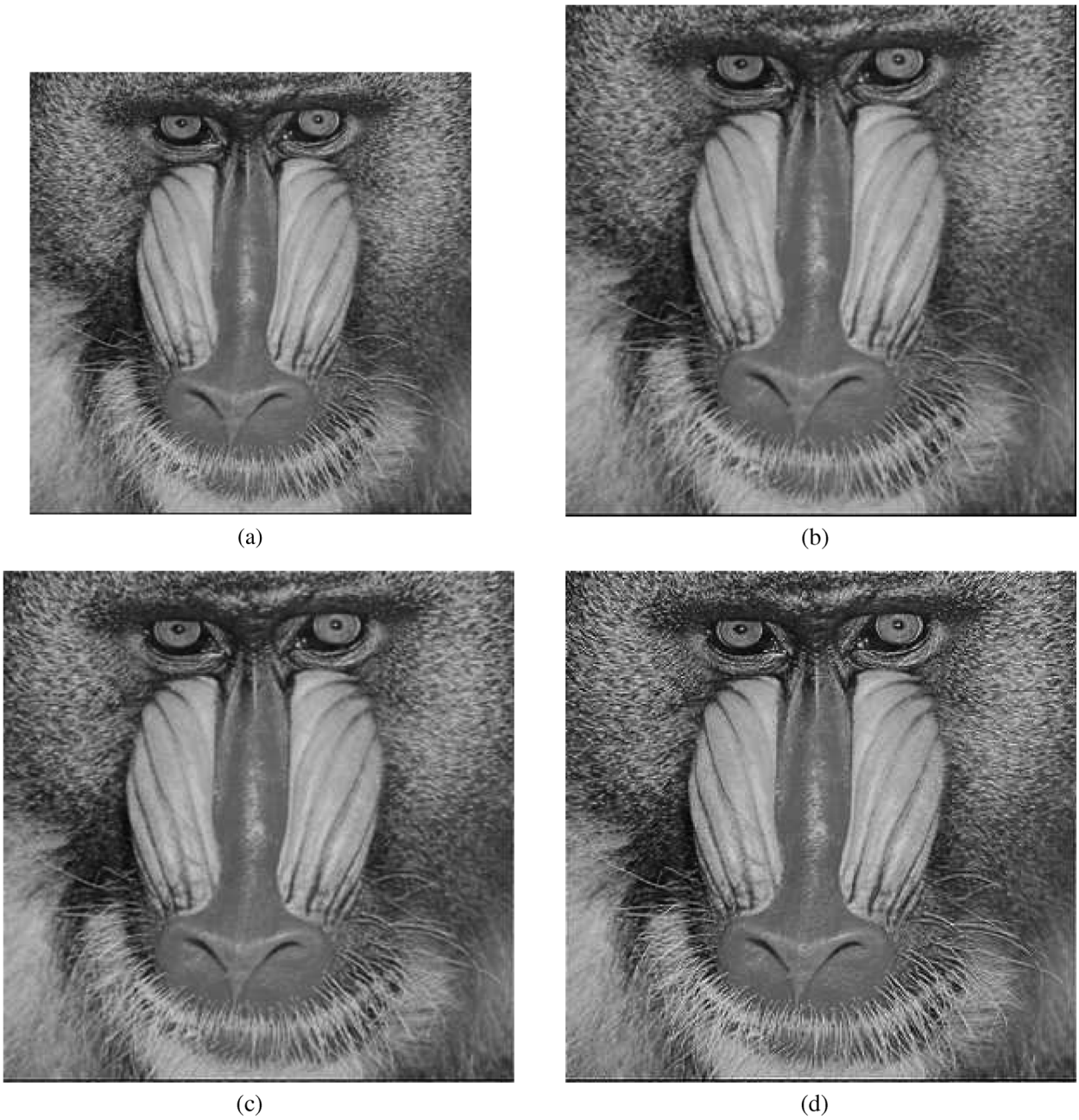


Fig. 12. (a) Original Mandrill image of size 256 × 256. (b) Enlargement by a factor of $\pi/e$ with bicubic interpolation. (c) Second-order approximation with a grid of 0.5 pixel spacing. (d) Our approach with a grid of 0.5 pixel spacing and linear interpolation.

where $\mathcal{F}\{R_{cd}[m,\cdot]\}(e^{iv})$ denotes the discrete-time Fourier transform of $R_{cd}[m,n]$ with respect to $n$ at frequency $v$. Now, taking the discrete Fourier transform of both sides of (72) with respect to $m$ leads to

$$\Lambda_{xx}(v)S(v)\delta(u+v) = W(v)\Lambda_{cd}(e^{iu},e^{iv}). \quad (73)$$

Since $d[n]$ is the output of a linear system operating on the WSS sequence $c[n]$, the cross spectrum $\Lambda_{cd}(e^{iu},e^{iv})$ can be expressed in terms of $\Lambda_{cc}(e^{iu})$ and the transfer function of the system, leading to

$$\Lambda_{xx}(v)S(v)\delta(u+v) = W(v)\Lambda_{cc}(e^{iu})H(e^{iv},e^{iu}). \quad (74)$$

Taking into account that the left-hand side of (74) is zero unless $u=-v$, we may write it as

$$\Lambda_{xx}(u)S^*(u)\delta(u+v) = W(v)\Lambda_{cc}(e^{iu})H(e^{iv},e^{iu}). \quad (75)$$

We first note that if for some frequency $u \in [-\pi,\pi]$ the term $\Lambda_{xx}(u+2\pi l)S^*(u+2\pi l)$ vanishes for every $l \in \mathbb{Z}$ then $\Lambda_{cc}(e^{iu}) = 0$ and (75) is satisfied. Hence, for frequencies outside $\Omega_c$ defined in (8), we have the freedom to choose $W(v)$ and $H(e^{iv},e^{iu})$ arbitrarily. Next, due to the periodicity of $H(e^{iv},e^{iu})$, it can be seen from (74) that for frequencies in $\Omega_c$ the filter $W(\omega)$ must be chosen such that

$W(\omega) = \alpha(e^{i\omega})S(\omega)\Lambda_{xx}(\omega)$ for some nonvanishing $2\pi$-periodic function $\alpha(e^{i\omega})$. The transfer function $H(e^{iv}, e^{iu})$, then, must possess the form

$$H(e^{iv}, e^{iu}) = \frac{\sum_{n\in\mathbb{Z}} \delta(u+v-2\pi n)}{\Lambda_{cc}(e^{iu})\alpha(e^{iv})}, \quad v \in \Omega_c. \tag{76}$$

This expression has the structure of the frequency response of an LTI system. We conclude that in order for the pointwise MSE between $x(t)$ and $\widehat{x}(t)$ to be minimized, the correction system can only contain a time-varying component whose frequency response is nonzero outside $\Omega_c$. ∎

## APPENDIX B
## DERIVATION OF THE MATRIX $\boldsymbol{G}(e^{i\omega})$ AND VECTOR $\boldsymbol{v}(e^{i\omega})$

In this appendix, we derive the expressions for $\boldsymbol{G}(e^{i\omega})$ and $\boldsymbol{v}(e^{i\omega})$ in (30). Throughout the derivations we make use of the following identity:

$$\mathcal{F}\{x[n]\}(\omega) = \sum_{l\in\mathbb{Z}} X(\omega_l). \tag{77}$$

### A. The Matrix $\boldsymbol{G}(e^{i\omega})$

The $(l,r)$ entry in the infinite matrix $g_{m,n}$ depends on the signals $y_{r,n}(t)$ and $y_{l,m}(t)$ via (34). The definition of $y_{l,m}(t)$ is given by (24)

$$y_{l,m}(t) = \sum_{j\in\mathbb{Z}} \widetilde{w}_{t,m}[-j]c[j-l] \tag{78}$$

where the sequence $\widetilde{w}_{t,m}[j]$, which depends on the continuous parameter $t$ and on the integer index $m$, is defined as

$$\widetilde{w}_{t,m}[j] \triangleq w\left(t+j-\frac{m}{K}\right). \tag{79}$$

Substituting (78) in (34) leads to

$$\begin{aligned} g_{m,n}[l,r] &= E\left[\int_{t_0}^{t_0+1} \sum_{k\in\mathbb{Z}} \widetilde{w}_{t,n}[k]c[-k-r] \sum_{j\in\mathbb{Z}} \widetilde{w}_{t,m}[j]c[-j-l]dt\right] \\ &= \int_{t_0}^{t_0+1} \sum_{j\in\mathbb{Z}}\sum_{k\in\mathbb{Z}} R_{cc}[j-k+l-r]\widetilde{w}_{t,n}[k]\widetilde{w}_{t,m}[j]dt \\ &= \int_{t_0}^{t_0+1} \left(R_{cc}[j] * \widetilde{w}_{t,m}[-j] * \widetilde{w}_{t,n}[j]\right)[l-r]dt. \end{aligned} \tag{80}$$

It is evident from (80) that $g_{m,n}$ is an infinite Toeplitz matrix as its $(l,r)$ entry is only a function of $l-r$. As such, it corresponds to convolution with the sequence $g_{m,n}[j]$ defined by

$$g_{m,n}[j] = \int_{t_0}^{t_0+1} \left(R_{cc}[j] * \widetilde{w}_{t,m}[-j] * \widetilde{w}_{t,n}[j]\right) dt. \tag{81}$$

Let us write an explicit expression for the DTFT of $g_{m,n}[j]$

$$G_{m,n}(e^{i\omega}) = \Lambda_{cc}(e^{i\omega}) \int_{t_0}^{t_0+1} \widetilde{W}^*_{t,m}(e^{i\omega})\widetilde{W}_{t,n}(e^{i\omega})dt. \tag{82}$$

Using (77),

$$\Lambda_{cc}(e^{i\omega}) = \sum_{l\in\mathbb{Z}} |S(\omega_l)|^2 \Lambda_{xx}(\omega_l). \tag{83}$$

The Fourier transform of $\widetilde{w}_{t,m}[n]$ is given by

$$\begin{aligned} \widetilde{W}_{t,m}(e^{i\omega}) &= \sum_{n\in\mathbb{Z}} w\left(t+n-\frac{m}{K}\right) e^{-i\omega n} \\ &= \sum_{k\in\mathbb{Z}} W(\omega_k) e^{i\omega_k\left(t-\frac{m}{K}\right)} \end{aligned} \tag{84}$$

where the last row is, again, obtained from (77). Finally

$$\int_{t_0}^{t_0+1} \widetilde{W}^*_{t,m}(e^{i\omega})\widetilde{W}_{t,n}(e^{i\omega})dt = \sum_{l\in\mathbb{Z}} |W(\omega_l)|^2 e^{i\omega_l\left(\frac{m-n}{K}\right)} \tag{85}$$

where we used the identity

$$\int_{t_0}^{t_0+1} e^{i2\pi t(l-k)}dt = \delta_{k,l}. \tag{86}$$

Substituting (83) and (85) into (82) we have

$$G_{m,n}(e^{i\omega}) = \sum_{l\in\mathbb{Z}} |S(\omega_l)|^2 \Lambda_{xx}(\omega_l) \sum_{l\in\mathbb{Z}} |W(\omega_l)|^2 e^{i\omega_l\left(\frac{m-n}{K}\right)}. \tag{87}$$

### B. The Vector $\boldsymbol{v}(e^{i\omega})$

The $l$th element in the sequence $v_m$ is given by (26). Substituting (24) of $y_{l,m}(t)$ into (26) leads to

$$\begin{aligned} v_m[l] &= E\left[\int_{t_0}^{t_0+1} x(t) \sum_{j\in\mathbb{Z}} w\left(t-j-\frac{m}{K}\right) c[j-l]dt\right] \\ &= \int_{t_0}^{t_0+1} \sum_{j\in\mathbb{Z}} \widetilde{w}_{t,m}[-j] E\left[x(t)c[j-l]\right] dt. \end{aligned} \tag{88}$$

This expression depends on the cross correlation of $x(t)$ and $c[n]$, which is given by

$$\begin{aligned} E\left[x(t)c[n]\right] &= E\left[x(t)\int_{-\infty}^{\infty} s(\tau-n)x(\tau)d\tau\right] \\ &= \int_{-\infty}^{\infty} s(\tau-n)R_{xx}(t-\tau)d\tau \\ &= \left(R_{xx}(t) * s(t)\right)(t-n) \triangleq Rs_t[n] \end{aligned} \tag{89}$$

where $Rs_t[n]$ is a sequence which depends on a continuous parameter $t$. Using (89) we may write (88) in terms of a discrete-time convolution

$$v_m[l] = \int_{t_0}^{t_0+1} \sum_{j\in\mathbb{Z}} \widetilde{w}_{t,m}[-j]Rs_t[j-l]dt = \int_{t_0}^{t_0+1} \left(\widetilde{w}_{t,m}[j] * Rs_t[j]\right)[-l]dt. \quad (90)$$

Now the DTFT of the sequence $v_m$ can be written explicitly

$$V_m(e^{i\omega}) = \int_{t_0}^{t_0+1} \widetilde{W}^*_{t,m}(e^{i\omega}) \sum_{l\in\mathbb{Z}} \Lambda_{xx}(\omega_l)S(\omega_l)e^{i\omega_l t}dt = \sum_{l\in\mathbb{Z}} \Lambda_{xx}(\omega_l)S(\omega_l) \int_{t_0}^{t_0+1} \widetilde{W}^*_{t,m}(e^{i\omega})e^{i\omega_l t}dt \quad (91)$$

where we used (77). Substituting the expression for $\widetilde{W}_{t,m}(\omega)$ from (84)

$$V_m(e^{i\omega}) = \sum_{l,k\in\mathbb{Z}} W^*(\omega_k)\Lambda_{xx}(\omega_l)S(\omega_l)e^{i\omega_k \frac{m}{K}} \cdot \int_{t_0}^{t_0+1} e^{i2\pi l(l-k)t}dt = \sum_{l\in\mathbb{Z}} W^*(\omega_l)\Lambda_{xx}(\omega_l)S(\omega_l)e^{i\omega_l \frac{m}{K}} \quad (92)$$

where we used (86).

## REFERENCES


[1] A. Balakrishnan, "A note on the sampling principle for continuous signals," *IEEE Trans. Inf. Theory*, vol. 3, no. 2, pp. 143–146, 1957.

[2] S. Lloyd, "A sampling theorem for stationary (wide sense) stochastic processes," *Trans. Amer. Math. Soc.*, vol. 92, no. 1, pp. 1–12, 1959.

[3] F. O. Huck, C. L. Fales, N. Halyo, R. W. Samms, and K. Stacy, "Image gathering and processing—Information and fidelity," *Opt. Soc. Amer. J. A: Opt. Image Sci.*, vol. 2, pp. 1644–1666, 1985.

[4] M. Matthews, "On the linear minimum-mean-squared-error estimation of an undersampled wide-sense stationary random process," *IEEE Trans. Signal Process.*, vol. 48, no. 1, pp. 272–275, 2000.

[5] S. Ramani, D. Van De Ville, and M. Unser, "Sampling in practice: Is the best reconstruction space bandlimited?," in *Proc. 2005 IEEE Int. Conf. Image Process. (ICIP'05)*, Genova, Italy, Sep. 11–14, 2005, vol. II, pp. 153–156.

[6] C. A. Glasbey, "Optimal linear interpolation of images with known point spread function," in *Scandinavian Image Analysis Conf. -SCIA-2001*, 2001, pp. 161–168.

[7] S. Ramani, D. Van De Ville, and M. Unser, "Non-ideal sampling and adapted reconstruction using the stochastic Matern model," in *Proc. Int. Conf. Acoust., Speech, Signal Process. (ICASSP'06)*, 2006, vol. 2.

[8] C. L. Fales, F. O. Huck, J. Mccormick, and S. Park, "Wiener restoration of sampled image data-end-to-end analysis," *Opt. Soc. Amer. J., A: Opt. Image Sci.*, vol. 5, pp. 300–314, 1988.

[9] M. Unser and A. Aldroubi, "A general sampling theory for nonideal acquisition devices," *IEEE Trans. Signal Process.*, vol. 42, no. 11, pp. 2915–2925, 1994.

[10] Y. C. Eldar and T. G. Dvorkind, "A minimum squared-error framework for generalized sampling," *IEEE Trans. Signal Process.*, vol. 54, no. 6, pp. 2155–2167, 2006.

[11] Y. C. Eldar and T. Werther, "General framework for consistent sampling in Hilbert spaces," *Int. J. Wavelets, Multiresolution, Inf. Process.*, vol. 3, no. 3, pp. 347–359, 2005.

[12] T. Dvorkind and Y. C. Eldar, "Robust and consistent solutions for generalized sampling," *IEEE Signal Process. Lett.*, 2007, submitted for publication.

[13] Y. C. Eldar and M. Unser, "Nonideal sampling and interpolation from noisy observations in shift-invariant spaces," *IEEE Trans. Signal Process.*, vol. 54, no. 7, pp. 2636–2651, 2006.

[14] J. G. Proakis and D. G. Manolakis, *Digital Signal Processing: Principles, Algorithms, and Applications*. Upper Saddle River, NJ: Prentice-Hall, 1996.

[15] N. Wiener, *Extrapolation, Interpolation and Smoothing of Stationary Time Series*. Cambridge, MA: MIT Press, 1949.

[16] L. E. Franks, *Signal Theory*. Upper Saddle River, NJ: Prentice-Hall, 1969.

[17] T. Blu and M. Unser, "Quantitative Fourier analysis of approximation techniques. I. Interpolators and projectors," *IEEE Trans. Signal Process.*, vol. 47, no. 10, pp. 2783–2795, 1999.


**Tomer Michaeli** received the B.Sc. degree (*summa cum laude*) in electrical engineering in 2004 from the Technion-Israel Institute of Technology, Haifa.

He is currently pursuing the Ph.D. degree in electrical engineering at the Technion. From 2000 to 2008, he was a research engineer at RAFAEL Research Laboratories, Israel Ministry of Defense, Haifa. In 2008 he held the Andrew and Erna Finci Viterbi Fellowship. His research interests include statistical signal processing, estimation theory, sampling theory, image processing, and computer vision.

**Yonina C. Eldar** (S'98–M'02–SM'07) received the B.Sc. degree in physics in 1995, the B.Sc. degree in electrical engineering in 1996, both from Tel-Aviv University (TAU), Tel-Aviv, Israel, and the Ph.D. degree in electrical engineering and computer science in 2001 from the Massachusetts Institute of Technology (MIT), Cambridge.

From January 2002 to July 2002 she was a Postdoctoral Fellow with the Digital Signal Processing Group of MIT. She is currently an Associate Professor with the Department of Electrical Engineering at the Technion—Israel Institute of Technology, Haifa. She is also a Research Affiliate with the Research Laboratory of Electronics at MIT. Her research interests are in the general areas of signal processing, statistical signal processing, and computational biology.

Dr. Eldar was in the program for outstanding students at TAU from 1992 to 1996. In 1998, she held the Rosenblith Fellowship for study in Electrical Engineering at MIT, and in 2000, she held an IBM Research Fellowship. From 2002–2005 she was a Horev Fellow of the Leaders in Science and Technology program at the Technion and an Alon Fellow. In 2004, she was awarded the Wolf Foundation Krill Prize for Excellence in Scientific Research, in 2005 the Andre and Bella Meyer Lectureship, in 2007 the Henry Taub Prize for Excellence in Research, and in 2008 the Hershel Rich Innovation Award, the Award for Women with Distinguished Contributions, and the Muriel and David Jacknow Award for Excellence in Teaching. She is a member of the IEEE SIGNAL PROCESSING THEORY AND METHODS technical committee and the Bio Imaging Signal Processing technical committee, an Associate Editor for the IEEE TRANSACTIONS ON SIGNAL PROCESSING, the EURASIP JOURNAL OF SIGNAL PROCESSING, and the SIAM *Journal on Matrix Analysis and Applications*, and on the Editorial Board of *Foundations and Trends in Signal Processing*.